Biomedicine & Pharmacotherapy 172 (2024) 116314

Contents lists available at ScienceDirect

Biomedicine & Pharmacotherapy

journal homepage: www.elsevier.com/locate/biopha

Chronic melatonin treatment improves obesity by inducing uncoupling of skeletal muscle SERCA-SLN mediated by CaMKII/AMPK/PGC1α pathway and mitochondrial biogenesis in female and male Zücker diabetic fatty rats

D. Salagre [a], M. Navarro-Alarcón [b], M. Villalón-Mir [b], B. Alcázar-Navarrete [c], G. Gómez-Moreno [d], F. Tamimi [e], A. Agil [a,*]

[a] Department of Pharmacology, BioHealth Institute Granada (IBs Granada), Neuroscience Institute (CIBM), School of Medicine, University of Granada, Granada 18016, Spain
[b] Department of Nutrition and Bromatology, School of Pharmacy, University of Granada, Granada 18071, Spain
[c] CIBERES, Carlos III Health Institute, Madrid, and Pulmonology Unit, Hospital Universitario Virgen de las Nieves, Granada 18014, Spain
[d] Department of Medically Compromised Patients in Dentistry, School of Dentistry, University of Granada, Granada 18011, Spain
[e] College of Dental Medicine, QU Health, Qatar University, Doha, Qatar

ARTICLE INFO

Keywords:
Zücker diabetic fatty rat
Obesity
Non-shivering thermogenesis
SERCA-SLN
CaMKII/AMPK/PGC1α
Mitochondrial biogenesis
Visceral fat

ABSTRACT

Melatonin acute treatment limits obesity of young Zücker diabetic fatty (ZDF) rats by non-shivering thermogenesis (NST). We recently showed melatonin chronically increases the oxidative status of *vastus lateralis* (VL) in both obese and lean adult male animals. The identification of VL skeletal muscle-based NST by uncoupling of sarcoendoplasmic reticulum Ca^{2+}-ATPase (SERCA)- sarcolipin (SLN) prompted us to investigate whether melatonin is a SERCA-SLN calcium futile cycle uncoupling and mitochondrial biogenesis enhancer. Obese ZDF rats and lean littermates (ZL) of both sexes were subdivided into two subgroups: control (C) and 12 weeks orally melatonin treated (M) (10 mg/kg/day). Compared to the control groups, melatonin decreased the body weight gain and visceral fat in ZDF rats of both sexes. Melatonin treatment in both sex obese rats restored the VL muscle skin temperature and sensitized the thermogenic effect of acute cold exposure. Moreover, melatonin not only raised SLN protein levels in the VL of obese and lean rats of both sexes; also, the SERCA activity. Melatonin treatment increased the SERCA2 expression in obese and lean rats (both sexes), with no effects on SERCA1 expression. Melatonin increased the expression of thermogenic genes and proteins (PGC1-α, PPARγ, and NRF1). Furthermore, melatonin treatment enhanced the expression ratio of P-CaMKII/CaMKII and P-AMPK/AMPK. In addition, it rose mitochondrial biogenesis. These results provided the initial evidence that chronic oral melatonin treatment triggers the CaMKII/AMPK/PGC1α axis by upregulating SERCA2-SLN-mediated NST in ZDF diabetic rats of both sexes. This may further contribute to the body weight control and metabolic benefits of melatonin.

1. Introduction

Enhancing energy expenditure is a promising strategy to reduce obesity. In homeothermic mammals, the skeletal muscle (SKM) is the largest organ and a main contributor to energy expenditure in adaptive temperature regulation by using muscle non-shivering thermogenesis (NST) [1]. SKM NST relies predominantly on futile calcium (Ca^{2+}) handling regulation by Sarco(endo)plasmic reticulum Ca^{2+}-ATPase (SERCA) [2–4]. SERCA maintains organellar and cytosolic Ca^{2+} levels and can be regulated by little peptides like Sarcolipin (SLN) that uncouples SERCA activity [1]. These uncoupling mechanisms regulated by SLN mediate muscle NST improving energy expenditure, and body weight loss [5,6]. SLN, as an uncoupler of SERCA, leads to the Ca^{2+} futile cycling of the pump, and enhances ATP hydrolysis and heat production, generating energy demand [7]. Also, an increase of cytosolic Ca^{2+} activates the Ca^{2+}-dependent signaling pathway and nuclear transcription factors promoting mitochondria biogenesis [8]. Augmented generation of new mitochondria constitutes a significant constituent of adaptive thermogenesis, particularly within brown adipose tissue (BAT) and skeletal musculature [9]. Peroxisome proliferator-activated receptor gamma (PPARγ) is a nuclear receptor that regulates mitochondrial biogenesis and oxidative metabolism in SKM together with its

* Correspondence to: Avda. del Conocimiento s/n, Granada 18016, Spain.
E-mail address: aagil@ugr.es (A. Agil).

https://doi.org/10.1016/j.biopha.2024.116314
Received 18 December 2023; Received in revised form 14 February 2024; Accepted 17 February 2024
Available online 22 February 2024

transcriptional coactivator the PPARγ coactivator 1-alpha (PGC1α), playing a vital role in adaptive thermogenesis by promoting the expression of genes involved in fatty acid oxidation and mitochondrial function, enhancing the energy expenditure, and reducing obesity [10,11]. PGC-1α elicits the enhancement of mitochondriogenesis through upregulating nuclear respiratory factor (NRF1), ultimately resulting in augmented mitochondrial DNA (mtDNA) replication and heightened respiratory gene transcription [12]. NRF1 is a transcription factor that controls mitochondrial biogenesis and oxidative metabolism in SKM, which may play a critical role in NST [13,14]. The thermogenic function of SLN is up-regulated by elevation of intracellular Ca^{2+} level [7] which can be stimulated by exercise training [15]. Citrate synthase (CS) is a key enzyme in the tricarboxylic acid cycle, which plays a vital role in oxidative metabolism and energy production [16]. SKM CS activity is regulated by various factors, including AMP-activated protein kinase (AMPK), which is a central regulator of cellular energy homeostasis [17]. AMPK is activated during energy stress [18] by Ca^{2+}-dependent pathways like Ca^{2+}/calmodulin (CaM)-dependent protein kinase II (CaMKII) and/or CaMKII kinase (CaMKKII) enhancing PGC1α expression and leading to increased energy expenditure, oxidative metabolism, and mitochondria biogenesis [19–21], being also a crucial pathway involved in the regulation of adaptive thermogenesis in SKM. Obesity is shown to disrupt cellular Ca^{2+} signaling affecting contractile function by decreasing muscle mass, force, power, and strength [22]. Also, these molecular changes affect Ca^{2+}-dependent pathways decreasing AMPK and PGC1-α activation resulting in a loss of the SKM metabolic control [22]. Interestingly, SKM NST can be activated in animals by physiological stimuli like cold exposure [23,24] and by several natural products limiting obesity [5]. Overall, understanding the various factors and mechanisms that regulate NST thermogenesis in SKM is crucial for developing effective therapy to treat obesity.

Melatonin is a neurohormone produced at night by the pineal gland [25,26] and also in many other tissues [27], which can also be found in numerous plant-derived foods, medicinal plants, vegetables, fruits, cereals, spices, and plant seeds [28,29]. Studies on female and male rats have reported that melatonin treatment curtails obesity without affecting feed intake and locomotor activity in part via the activation of thermogenesis of brown and beige adipose tissue [30–32]. However, those mechanisms alone seem to be insufficient to explain the 12% reduction in body weight elicited by melatonin. It has been recently proposed that melatonin may increase *vastus lateralis* (VL) muscle oxidative capacity in both obese and lean adult male ZDF rats [33]. However, direct proof of the thermogenic properties of the newly recruited VL muscle in response to melatonin is still lacking. Also, previous studies showed that melatonin increases intracellular Ca^{2+} levels in SKM revealing the tight connection between this indolamine and Ca^{2+} homeostasis [34,35]. Thus, in the present work, we investigated the potential role of orally chronic administrated melatonin on obesity and NST inducing Ca^{2+}-dependent thermogenic pathways in the VL muscle from both sex ZDF rats. Overall, the mechanisms linking melatonin to NST via SLN activation remain unexamined. For this purpose, we used male and female ZDF rats, a model of diabesity with type 2 diabetes mellitus (T2DM) similarity to human pathogenesis [36,37]. The ZDF rat model utilized in this study best mirrors the characteristics of the physiopathology of diabesity in humans, owing in part to the specific diet provided according to the manufacturer's instructions. This regimen results in both male and female rats becoming insulin-resistant and developing associated T2DM due to obesity [36,37]. Additionally, it is essential to consider that fat distribution in mammalian models differs across species and sexes. In humans, deep subcutaneous adipose tissue (dSAT) with similar characteristics to visceral adipose tissue (VAT) fat is closely related to obesity-associated complications and insulin resistance [38]. Similarly, in the ZDF rat, perigonadal and perirenal visceral fat depots are linked to glucose intolerance and insulin resistance [39]. Thus, the ZDF rat model faithfully represents the physiopathology and the sex-based differences observed in obese women where a higher visceral fat index was found [38]. We evaluated the effects of chronic treatment of melatonin on body weight gain, relative visceral fat weight, the expression of SLN, or/and the activity of both SERCA isoform 1 (SERCA1) and 2 (SERCA2). Also, we assessed the expression of thermogenic proteins such as PGC1α, PPARγ, and NRF1. We examined the effect of melatonin on the VL muscle skin temperature at rodent's thermoneutrality and after cold exposure, as a reflection of heat production in female and male (6–18 weeks old) ZDF rats.

2. Material and Methods

2.1. Animals and experimental protocol

This research was conducted following the ethical guidelines outlined by the European Union for the care and protection of animals and was approved by the Ethical Committee of the University of Granada (Granada, Spain) under permit project number 23/06/2021/096-CEEA. ZDF rats (fa/fa) from both sexes (male, N = 16; female, N = 16) and lean littermates (ZL, fa/-; male, N = 16; female, N = 16) were obtained at 5 weeks (wks) of age. Male animals were maintained on Purina #5008 rat chow (protein 23%, fat 14%, carbohydrates (by difference) 51%, fiber 4%, and ash 8%) and female on Research (protein 12%, fat 25.5%, carbohydrates (by difference) 51%, fiber 6% and ash 5.5%) and tap water ad libitum. The ZDF rats are widely acknowledged as a robust rodent model for studying the metabolic syndrome owing to their propensity to develop early and progressive obesity, dyslipidemia, hypertension, endothelial dysfunction, hyperinsulinemia, and hyperglycemia when maintained with the mentioned specific and manufacture's recommended diet for each sex, which closely mimic the clinical characteristics of human T2DM [40,41]. T2DM manifests in these rats at approximately 9–10 wks of age, followed by insulinopenic diabetes at around 20 wks of age [41,42]. The animals were housed in pairs in transparent plastic cages in a climate-controlled environment maintained at thermoneutrality (28–30 °C) and 30–40% relative humidity, with a light/dark cycle of 12 hours (lights on at 7 a.m.). During the initial week following their arrival, the animals were allowed to acclimatize to the room conditions, and their water intake was recorded. Subsequently, both male and female ZL and ZDF rats were divided into four groups: untreated control animals (male C-ZL and C-ZDF, and female C-ZL and C-ZDF; n = 8) and treated with oral melatonin (10 mg/kg/day) in drinking water with a final ethanol concentration of 0.066% v/v for 12 wks (male M-ZL and M-ZDF, and female M-ZL and M-ZDF; n = 8). Fresh melatonin was prepared every two days, and the melatonin dose was adjusted based on body weight (BW) and water consumption, recorded daily, throughout the study period. Water bottles were shielded with aluminum foil to safeguard against light exposure. At the end of the experimental protocol, the animals were anesthetized with sodium thiobarbital (thiopental) and euthanized. An incision was made at the ventral midline, exposing the abdominal cavity, and the gastrointestinal tract was removed through dissections above the stomach and at the base of the colon, exposing the internal fat pads. Retroperitoneal, perigonadal (testes or ovaries), and mesenteric fat pads were then removed. The mesenteric fat depot was removed from the length of the gut, with blood vessels and connective tissue included. The fat pads were weighed immediately after dissection to avoid evaporative weight loss. Estimates of visceral fat were calculated by summing intraabdominal fat pad (retroperitoneal, perigonadal, and mesenteric) weights and normalized to 100 g body weight (fat mass index, %) for central obesity determination.

2.2. Acute cold challenge

Melatonin administration was ceased 2 hours prior to the commencement of the experiment. The acute cold exposure was conducted between 09:00 and 11:00 hr, lasting 5 minutes. First, rats were anesthetized with 4% isoflurane for induction and 2.5% isoflurane for

maintenance using an anesthesia gas vaporizer (MSSVAP02, MSS International, United Kingdom). Then, the rats were placed on a hot/cold plate analgesia meter pre-cooled to 4°C (Series 8 Model PE34, IITC Life Science, USA). This apparatus consisted of a 16.5 × 16.5 cm metal plate capable of being cooled to −3°C or heated to 65°C. The plate's temperature was regulated by an electronic thermostat, and a front panel digital thermometer displayed the current temperature of the plate. Transparent plastic walls enclosed the plate, creating an environment with a temperature of approximately 10°C. Thermal images of the superficial VL regions were captured using a thermal imaging camera (E52, FLIR Systems AB, Sweden) with a temperature range spanning from −20°C to 120°C. Images were taken perpendicular to the region of interest at 20 cm of distance before the cold challenge (at thermoneutral temperature, 28–30 °C) and immediately afterwards (at 4°C). The temperature of the superficial VL skin was measured utilizing the thermal camera, which is capable of detecting even subtle changes in tissue temperature.

2.3. Total VL protein extraction and Protein expression analysis by Western-Blot

Proteins were extracted from approximately 0.5 g of the VL sample using RIPA Lysis Buffer (150 mM NaCl, 50 mM Tris-HCl, 1% Nonidet P-40, 0.5% sodium deoxycholate, and 0.1% sodium dodecyl sulfate (SDS)). To enhance the protein isolation process, 1% Triton X-100, 1% protease inhibitor cocktail, and 1% phosphatase inhibitor cocktail were added to the buffer. Homogenization was performed using a Teflon pestle (10 cycles of 6 seconds each) while maintaining a constant temperature of 4 °C throughout all procedures. The resulting homogenates were then subjected to centrifugation at a speed of 13,000 × g for a duration of 15 minutes at 4 °C. The supernatant, which appeared clear, was cautiously transferred to a new tube, and aliquots of the total protein lysate were preserved at −80 °C for subsequent Western blotting analysis. Protein concentration was determined using the Bradford method, employing bovine serum albumin (BSA) as the standard.

For the analysis of total protein extracts, 50 μg of protein was separated using SDS-polyacrylamide gel electrophoresis (SDS-PAGE). The gels were then transferred onto a nitrocellulose membrane (Bio-Rad Trans-Blot SD, Bio-Rad Laboratories, Hercules, CA, USA). Subsequently, the membranes were subjected to a blocking step (1 hour at room temperature (RT)) using Blocking Buffer (Phosphate Buffer Saline (PBS) containing 137 mM NaCl, 2.7 mM KCl, 10 mM Na2HPO4, and 1.8 mM KH2PO4, supplemented with 1% Tween-20 (PBS-T) and 5% non-fat dry milk). Overnight incubation was carried out at 4 °C with primary antibodies specifically raised in mice and rabbit against SERCA1 (cat#-SAB4502027, Sigma-Aldrich, Spain), SERCA2 (cat#S1439, Sigma-Aldrich, Spain), SLN (cat#MBS713457, MyBiosource, USA), PGC1α (cat#SAB2500781, Sigma-Aldrich, Spain), PPARγ (cat#A-V32880–100UL, Sigma-Aldrich, Spain), AMPK (cat#SAB4502329, Sigma-Aldrich, Spain), P-AMPK (cat#SAB4503754, Sigma-Aldrich, Spain), Calmodulin (cat#SC-137079, Santa Cruz Biotechnology, USA), CaMKII (cat#SC-13141, Santa Cruz Biotechnology, USA), P-CaMKII (cat#SC-32289, Santa Cruz Biotechnology, USA), CaMKKII (cat#PA5–78909, Thermofisher Scientific, Spain), and P-CaMKKII (cat#PA5–105225, Thermofisher Scientific, Spain) at dilutions of 1:1000 in the PBS-T with 10% Blocking Buffer. An anti-β-actin antibody, generated in mice (cat#SC-81178; Santa Cruz Biotechnology, USA), was utilized at a dilution of 1:1000 in the PBS-T with 10% Blocking Buffer as a loading control. Following overnight incubation, the membranes underwent three 15-minute washes in PBS-T to eliminate any unbound primary antibodies. Subsequently, the membranes were incubated at room temperature for 2 hours with respective horseradish peroxidase (HRP)-conjugated secondary antibodies (cat#A16035, Donkey anti-Rabbit IgG, Thermofisher Scientific, Spain; cat#MBS674947, Donkey Anti-Mouse IgG, MyBiosource, USA) at a dilution of 1:2000 in the PBS-T with 10% Blocking Buffer. After three additional 15-minute washes in PBS-T, immunoreactive proteins were detected using the Clarity Western ECL commercial kit (BioRad, Spain) following the manufacturer's instructions. Signal intensities were captured using the Image Station 4000MM Pro Molecular Imaging system (Kodak, USA) and quantitatively analyzed using Image J 1.33 software (National Institutes of Health, Bethesda, MD, USA). The obtained results were normalized to β-actin amounts. All experiments were performed in triplicate.

2.4. Total VL RNA extraction and gene expression analysis by reverse transcriptase-quantitative-polymerase chain reaction (RT-q-PCR)

Approximately 25 mg of VL tissue was used to extract total RNA employing the RNeasy Mini Kit (cat#74104, QIAGEN, Germany). The integrity and quantity of the isolated RNA were assessed by spectrophotometric absorption at 230, 260 and 280 nm using a Nanodrop One/One (cat#ND-ONE-W, Thermofisher Scientific, Spain).

Subsequently, 1.0 μg of RNA was utilized for the synthesis of first-strand cDNA by GoScript Reverse Transcriptase Kit (cat#A5001, Promega, USA). The RT process was conducted in a final 20 μL reaction volume.

For q-PCR, GoTaq qPCR Master Mix (cat#A6002, Promega, USA) was used following manufacturer's protocol and amplification was measured in a QuantStudio 3 Real-Time PCR System thermocycler (cat#A28567, Thermofisher Scientific, Spain). The primers used for amplifying the target genes (PPARG, PPARGC1A, NRF1) were generated using Primer-Blast platform from National Center for Biotechnology Information (NCBI) and listed in Table 1. Amplification of β-actin (ACTB) cDNA was used as an internal control. To ensure PCR linearity and validate cDNA quantitation, appropriate controls and standard curves were performed by amplifying first-strand cDNA for 16–31 cycles. The amplified products were separated on a 1% agarose gel and stained with Sybr Safe (cat#S33102, Thermofisher Scientific, Spain) for verifying RT-q-PCR quality.

2.5. Genomic DNA extraction and mitochondrial DNA copy number analysis

Approximately 25 mg of VL tissue was used to extract genomic DNA employing the DNeasy Blood and Tissue Kit (cat#69504, QIAGEN, Germany). The integrity and quantity of the isolated DNA were assessed by spectrophotometric absorption at 230, 260 and 280 nm using a Nanodrop One/One (cat#ND-ONE-W, Thermofisher Scientific, Spain).

Genomic DNA was digested by *Xho*I restriction enzyme (cat#R0146L, New England Biolabs, USA) using 20 units of enzyme per μg of genomic DNA in 1 hour digest at 37°C in a total reaction volume of 50 μl. After digestion, enzyme was inactivated by incubation at 65°C for 20 minutes.

mtDNA copy number was measured by taking ratio between a target mitochondrial gene and a reference nuclear gene (mtDNA /nDNA) using q-PCR as previously described. The primers used for amplifying the mitochondrial target gene (MT-RNR2) were listed in Table 1. Amplification of GAPDH was used as an internal control of nuclear DNA copy number. The amplified products were separated on a 1% agarose gel and stained with Sybr Safe (cat#S33102, Thermofisher Scientific, Spain) for verifying q-PCR quality.

2.6. Mitochondrial isolation and CS activity measurement

VL samples, weighing approximately 300 mg, were dissected. Mitochondria were subsequently isolated from this tissue using a sequential centrifugation technique following a previously reported protocol, that has the advantage of preserving the integrity of the mitochondrial membrane, with minor adaptations [43]. The excised tissues were thoroughly rinsed with cold saline and homogenized in an isolation medium (IM) composed of 10 mM Tris, 250 mM sucrose, 0.5 mM Na2EDTA, and 1 g/L BSA with free fatty acids (pH 7.4, 4 °C),

Table 1
List of primers pair used in RT-q-PCR and mitochondrial DNA copy number measurements.

Gene	Forward sequence (5' → 3')	Reverse sequence (5' → 3')
PPARG	CACAATGCCATCAGGTTTGGG	CAAATGCTTTGCCAGGGCTC
PPARGC1A	TATGGAGTGACATAGAGTGTGCT	GTCGCTACACCACTTCAATCC
NRF1	TACAAGGCGGGGGACAGATA	TGAACTCCATCTGGGCCATT
ACTB	ACCCGCCACCAGTTCGCCAT	CGGCCCACGATGGAGGGGAA
MT-RNR2	AATGGTTCGTTTGTTCAACGATT	AGAAACCGACCTGGATTGCTC
GAPDH	TGGCCTCCAAGGAGTAAGAAAC	GGCCTCTCTCTTGCTCTCAGTATC

using a Teflon pestle (4 cycles of 6 seconds each). The resulting homogenate was subjected to centrifugation at 1000× g for 10 minutes at 4 °C, followed by centrifugation of the supernatant at 15,000× g for 20 minutes at 4 °C. The resulting pellet was resuspended in 1 mL of IM devoid of BSA, and a portion of the suspension was frozen for subsequent determination of protein concentration using the Bradford method. The remaining mitochondrial suspensions were then subjected to centrifugation at 15,000× g for 20 minutes at 4 °C, followed by resuspension in 1 mL of 1x Assay Buffer for CS (cat#B6935, Sigma-Aldrich, Spain). The mitochondrial suspensions were kept on ice for 10–15 minutes before further experiments.

CS activity analysis was performed in isolated mitochondrial from VL using a CS Assay Kit (cat#CS0720, Sigma-Aldrich, Spain) following manufacturer's protocol in a 96-well plate and measuring the absorbance at 412 nm in the plate reader spectrophotometer Infinite F200 (TECAN, Swiss). CS activity was expressed as nmol/min/mg protein.

2.7. Endoplasmic reticulum (ER) isolation and sarcoendoplasmic reticulum Ca^{2+}-ATPase (SERCA) activity measurement

For ER isolation, approximately 0.5 g of VL were homogenized in the IM with a Teflon pestle (4 cycles of 6 seconds each). The homogenate was centrifuged at 1000× g for 10 minutes at 4 °C, followed by centrifugation of the supernatant at 15,000× g for 20 minutes at 4 °C. Finally, the supernatant was centrifuged at 100,000x g for 1 hour at 4 °C and the resulting pellet was resuspended in 1 mL of IM without BSA. An aliquot of the suspension was frozen for subsequent determination of protein concentration using the Bradford method. The remaining ER suspensions were then centrifuged at 100,000× g for 1 hour at 4 °C, followed by resuspension in 100 μL of incubation medium (80 mM KCl, 25 mM MOPS, 3 mM MgCl2, 5 mM sodium azide, pH 7.4).

SERCA activity was measured in ER and mitochondria isolated from VL samples through a spectrophotometric method based on the formation of a complex coordinated with phosphate ion that is released as a product of ATP hydrolysis (antimony-phosphomolybdate complex), generating a characteristic blue coloration also known as molybdate blue whose absorbance can be measured at 850 nm [44,45]. The rate of phosphate release serves us as a direct measure of the Ca^{2+}-ATPase activity. To start reaction, 50 μg of isolated ER or mitochondria were incubated 5 minutes at 37 ºC in 100 μl of incubation medium supplemented with 2 mM ATP and 0.4 mM CaCl2. After incubation, 900 μl of coloring solution (40 μM Potassium Antimony Tartrate, 0.5 mM Ammonium Molybdate, 125 mM H2SO4 and 10 mM Ascorbic Acid) were added to samples and absorbance was measured at 850 nm. Control experiments of SERCA activity were performed in the presence of 1 μM thapsigargin.

2.8. Statistical analysis

All experiments were conducted in triplicate, with each experiment being repeated at least twice in each rat to enhance the robustness of the findings. The results were presented as means ± standard deviation (SD) values. Comparative analyses between experimental groups were performed using a one-way analysis of variance (ANOVA), followed by the post-hoc Tukey's Test. Statistical significance was attributed to differences between groups when the *P*-value was less than 0.05. Statistical data analyses were carried out using SPSS version 22 for Windows (SPSS, Michigan, IL, USA).

3. Results

3.1. Effects of melatonin on BW and central obesity

To evaluate the effectiveness of melatonin against obesity, we first tested its effect on final body weight (FBW), body mass index (BMI), and normalized body weight gain (BW gain). The effects of melatonin on FBW (g), BMI (Kg/m^2), and BW gain (g/100gBW) are shown in Table 2 and Fig. 1. No difference in initial weights before the start of the experiments at 6 wks of life was observed between the two phenotypes of the same sex, nor between sexes. As expected, after the 12 wks of the experimental period, FBW, BW gain, and BMI were significantly greater in the C-ZDF (female, 342.6 ± 11; 62.97±4.43; 6.32±0.1; and male, 432.2 ± 3; 85.67±1.15; 6.44±0.05, respectively) compared to C-ZL of both sex animals (female, 252.2±9; 40.73±3.38; 4.41± 0.4; and male, 356.6±13; 69.09±5.22; 5.02±0.07, $P < 0.01$) (Table 2, Fig. 1). Also, male C-ZDF rats presented higher FBW and BW gain compared to female ones (male, 432.2 ± 3; 85.67±1.15, and female, 342.6 ± 11; 62.97 ±4.43, respectively; $P < 0.05$; Table 2 and Fig. 1). As expected, the food intake was higher in both sex ZDF than in ZL rats with no differences between sexes (Supplementary material Table 1).

The melatonin treatment significantly reduced the FBW, BW gain, and BMI in ZDF rats (female, to 297.9±6; 52.06±2.33; 5.12±0.3; male, to 374.6±6; 71.95±2.22; 5.69±0.34; $P < 0.05$) also as well significantly in ZL ones in the following parameters (female BMI, to 3.97 ±0.07; male FBW, to 316±3 and BW gain to, 59.14±3.00; $P < 0.05$; Table 2 and Fig. 1) and with no effects in others. The food intake was not influenced by melatonin treatment in either group (Supplementary material Table 1).

After that, to identify whether the melatonin treatment effected central specific white adipose depots, we weighed total VAT from visceral different anatomical locations; retroperitoneal adipose tissue (RAT), perigonadal adipose tissue (PAT), and mesenteric adipose tissue

Table 2
Initial body weight, final body weight, and final body mass index in both ZL and Zücker diabetic fatty (ZDF) groups of both sex female and male groups: control and melatonin-treated. Results were expressed as the mean and S.E.M., respectively (n = 8). One-way ANOVA followed by Tukey's post- test, (*$P < 0.05$ melatonin vs control rats; $^{\#\#}P < 0.01$ C-ZDF vs C-ZL rats; †$P < 0.05$ female C-ZDF vs male C-ZDF).

Sex	Phenotypes	Initial Body Weight (g)	Final Body Weight (g)	Final Body Mass Index (Kg/m2)
Female	C-ZL	98.3 ± 16	252.2 ± 9	4.41 ± 0.04
	M-ZL	102.4 ± 9	251.0 ± 5	3.97 ± 0.07 *
	C-ZDF	104.6 ± 12	342.6 ± 11 ##	6.32 ± 0.10 ##
	M-ZDF	101.1 ± 16	297.9 ± 6 *	5.12 ± 0.31 *
Male	C-ZL	95.4 ± 22	356.6 ± 13	5.02 ± 0.07
	M-ZL	92.7 ± 20	316.3 ± 8 *	5.06 ± 0.15
	C-ZDF	108.4 ± 17	432.2 ± 3 ## †	6.44 ± 0.05 ##
	M-ZDF	102.6 ± 23	374.6 ± 6 *	5.69 ± 0.34 *

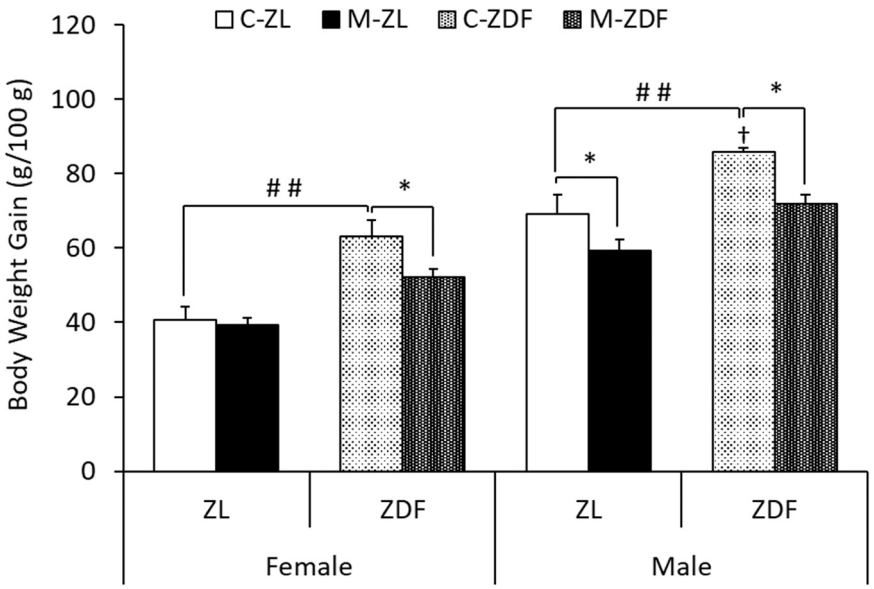

Fig. 1. Body weight gain in female and male ZL and Zücker diabetic fatty (ZDF) animals: control and melatonin-treated. Values are the means ± S.E.M. of 8 animals/group. Values not sharing a common superscript letter are significantly different by ANOVA/LSD (*$P < 0.05$ melatonin vs control rats; ##$P < 0.01$ C-ZDF versus C-ZL rats; †$P < 0.05$ female C-ZDF vs male C-ZDF).

(MAT), we precisely tested its effect in central obesity or visceral adiposity as expressed by VAT (g) and its adjusted index (VAT I) (% g BW) (Table 3). As expected, after the 12 wks of the experimental period, not only VAT and VAT I were significantly greater in the C-ZDF (female, 44.64 ± 2.06; 13.03 ± 0.41; and male, 49.3±2.081; 11.41±0.15) compared to C-ZL of both sex animals (female, 7.83±0.6; 3.1± 0.013; and male, 11.36±0.85; 3.18±0.17, $P < 0.01$; respectively) (Table 3), also as well, fat mass and index were higher in both sex obese rats compared to lean regarding to RAT (female, 21.12±0.93 and 6.16±0.18 vs 3.5±1.12 and 1.39±0.22; male, 24.05±2.82 and 5.56±0.3 vs 4.56 ±0.54 and 1.28±0.1), PAT (female, 16.88±1.06 and 4.93±0.21 vs 2.42 ±0.32 and 0.96±0.06; male, 20.36±1.61 and 4.71±0.3 vs 4.51±0.7 and 1.26±0.13) and MAT (female, 6.61±0.64 and 1.93±0.12 vs 1.85±0.29 and 0.73±0.15; male, 5.55±0.7 and 1.28±0.12 vs 2.2±0.51 and 0.62 ±0.1; $P < 0.01$) visceral fat pads. Furthermore, female C-ZDF rats presented increased VAT and MAT index compared to male C-ZDF ones (female, 13.03 ± 0.41 and 1.93±0.12 vs. male, 11.41±0.15 and 1.28 ±0.12, respectively; $P < 0.05$; Table 3).

Melatonin treatment significantly dropped both VAT and its index in both phenotype and sex rat (female; obese M-ZDF, 34.5±0.14; 11.58 ±0.02, $P < 0.01$; and lean M-ZL 6.43±0.4; 2.56±0.08, $P < 0.05$; male M-ZDF, 26.16±1.01; 6.98±0.2, $P < 0.01$; and M-ZL 8.74±0.61; 2.76±0.13, $P < 0.05$), by decreasing the RAT and its index (female M-ZDF, 19.25 ±0.21; 4.47±0.14, $P < 0.01$; and M-ZL fat index 0.98±0.0.05, $P < 0.05$; male M-ZDF, 13.47±1.05; 3.59±0.21, $P < 0.01$; and M-ZL fat index 0.94 ±0.2, $P < 0.05$) and also PAT (female M-ZDF, 9.49±0.61; 3.18±0.12; and male M-ZDF, 8.75±0.29; 2.33±0.09; $P < 0.01$) mass and its index with no effects in mesenteric visceral fat pad (Table 3).

3.2. *Effects of melatonin on VL thermogenic activity*

SKM plays an important role in thermoregulation and functions as thermogenic tissue. Consequently, an association is anticipated between the temperature of the superficial skin and the thermogenic activity of

Table 3
Mass (g) and relative mass index of the total visceral (TVAT), retroperitoneal (RAT), perigonadal (PAT), and mesenteric (MAT) adipose tissues of rats from both ZL and Zücker diabetic fatty (ZDF) groups of both sex female and male groups: control and melatonin. The values in the columns represent the mean and S.E.M., respectively (n = 8). One-way ANOVA followed by Tukey's post- test, (*$P < 0.05$ and **$P < 0.01$ melatonin vs control rats; ##$P < 0.01$ C-ZDF vs C-ZL rats; †$P < 0.05$ female C-ZDF vs male C-ZDF).

Sex	Phenotypes	Visceral AT: Fat index (%) Fat mass (g)	Retroperitoneal AT: Fat index (%) Fat mass (g)	Perigonadal AT: Fat index (%) Fat mass (g)	Mesenteric AT: Fat index (%) Fat mass (g)
Female	**C-ZL**	3.1 ± 0.13 7.83 ± 0.6	1.39 ± 0.22 3.5 ± 1.12	0.96 ± 0.06 2.42 ± 0.32	0.73 ± 0.15 1.85 ± 0.29
	M-ZL	2.56 ± 0.08 * 6.43 ± 0.4 *	0.98 ± 0.05 * 2.46 ± 0.15	1 ± 0.06 2.52 ± 0.31	0.57 ± 0.12 1.43 ± 0.12
	C-ZDF	13.03 ± 0.41 ## 44.64 ± 2.06 ##	6.16 ± 0.18 ## 21.12 ± 0.93 ##	4.93 ± 0.21 ## 16.88 ± 1.06 ##	1.93 ± 0.12 ## 6.61 ± 0.64 ##
	M-ZDF	11.58 ± 0.02 ** 34.5 ± 0.14 **	4.47 ± 0.14 ** 19.25 ± 0.21 **	3.18 ± 0.12 ** 9.49 ± 0.61 **	1.94 ± 0.06 5.79 ± 0.35
Male	**C-ZL**	3.18 ± 0.17 11.36 ± 0.85	1.28 ± 0.1 4.56 ± 0.54	1.26 ± 0.13 4.51 ± 0.7	0.62 ± 0.1 2.2 ± 0.51
	M-ZL	2.76 ± 0.13 * 8.74 ± 0.61 *	0.94 ± 0.2 * 2.97 ± 1.01	1.16 ± 0.12 3.67 ± 0.59	0.61 ± 0.09 1.93 ± 0.45
	C-ZDF	11.41 ± 0.1 ## † 49.3 ± 3.08 ##	5.56 ± 0.3 ## 24.05 ± 2.82 ##	4.71 ± 0.3 ## 20.36 ± 2.61 ##	1.28 ± 0.12 ## † 5.55 ± 0.7 ##
	M-ZDF	6.98 ± 0.2 ** 26.16 ± 1.01 **	3.59 ± 0.21 ** 13.47 ± 1.05 **	2.33 ± 0.09 ** 8.75 ± 0.29 **	1.13 ± 0.16 4.25 ± 0.19

the subjacent VL muscle. That is why thermal images were taken to test melatonin's effect on the VL thermogenic activity. As illustrated in Fig. 2, the temperature (ºC) of the skin underlying the VL muscle of C-ZDF rats and the response to cold challenge were lower in both sexes (female, 33.91±0.37; 0.17± 0.03; and male, 34.36±0.19; 0.13±0.04, respectively) compared to C-ZL ones (female, 35.23±0.36; 0.82± 0.09; and male, 35.12±0.22; 0.76±0.02; basal skin temperature, $P < 0.05$; cold challenge, $P < 0.01$). 12 weeks of prolonged administration of melatonin restored the superficial skin temperature in both sex obese rats (female, 34.89±0.34; and male, 35.02±0.25; $P < 0.05$). Melatonin additionally heightened the response to cold exposure, leading to an increase in superficial skin temperature in both sex ZDF rats (female, 0.47±0.02; and male, 0.66±0.0.07; $P < 0.01$) as well in male ZL rats (1.02±0.06; $P < 0.05$; Fig. 2).

3.3. Effects of melatonin on VL SERCA-SLN uncoupling

One of the recently discovered molecular signatures leading to thermogenic activity in SKM is the uncoupling of SERCA activity mediated by SLN. Therefore, we quantified the protein expression of SLN and SERCA isoforms, along with SERCA activity, in extracts from the VL muscle of both sex lean and obese rats following melatonin treatment, performing Western blot and spectrophotometry techniques, respectively. As expected from the thermal images, SLN and SERCA activity (nmol Pi/min/mg protein) were observed to be diminished in untreated obese animals from both sexes (female, 0.31±0.03; 25.67 ±2.21; and male, 0.36±0.04; 11.1±0.92, respectively) compared to lean control littermates (female, 0.54±0.04; 33.36±3.04; and male, 0.66 ±0.02; 18.98±0.72; SLN, $P < 0.01$; SERCA activity, $P < 0.05$), and melatonin treatment completely recovered (female, 0.51±0.03; 36.9 ±1.99; and male, 0.61±0.04; 17.73±0.55; SLN, $P < 0.01$; SERCA activity, $P < 0.05$), and even increasing them in both sex ZL treated rats (female SLN, 0.84±0.03, $P < 0.01$; and SERCA activity, 43.61±1.74, $P < 0.05$; and male SLN, 0.8±0.02, $P < 0.05$; and SERCA activity, 27.21 ±0.75, $P < 0.01$; Fig. 3A, B). Furthermore, female ZDF rats presented higher SERCA activity compared to males (female, 25.67±2.21 vs. male, 11.1±0.92; $P < 0.05$; Fig. 3B). Concerning SERCA isoforms expression, SERCA2 expression was lower in VL from both sex ZDF rats (female, 1.59 ±0.19; and male, 1.93±0.18) compared to their lean control animals (female, 2.63±0.16; and male, 2.86±0.11; $P < 0.05$). No differences in SERCA1 expression were observed between the two phenotypes, nor between sexes (Fig. 3D). Melatonin was shown to restore basal expression in VL from both sex ZDF rats (female, 2.41±0.17; and male, 2.68 ±0.12; $P < 0.05$) also increasing SERCA 2 expression in ZL rats (female, 4.05±0.37; and male, 3.76±0.09; $P < 0.05$; Fig. 3C). This thermogenic effect of melatonin increasing SLN and SERCA expression is also apparent in the blots shown in Fig. 3E.

3.4. Effects of melatonin on VL activation of Ca^{+2}-dependent thermogenic pathway

As the main function of SERCA is Ca^{+2} transport from the cytosol into the endoplasmic reticulum, to determine whether SERCA-SLN uncoupling mediated by melatonin treatment may regulate the Ca^{2+}-dependent thermogenic pathway, we performed a western blot technique to measure the activation (by phosphorylation) of different proteins involved in this thermogenic Ca^{+2}-dependent molecular signaling cascade. Obese-diabetic rats from both sexes presented lower levels of CaM expression (female, 0.11±0.010; male, 0.08±0.014) compared to their respective lean control female (0.16±0.012; $P < 0.05$) and male animals (0.17±0.002; $P < 0.01$). After melatonin treatment, CaM expression in the VL muscle was increased in both sex and phenotype animals (female M-ZDF, 0.31±0.008; and M-ZL, 0.29±0.015; male M-ZDF, 0.16±0.009; and M-ZL, 0.29±0.03; $P < 0.01$; Fig. 4A). The P-CaMKKII/CaMKKII ratio was also decreased in both sex ZDF rats (female: C-ZDF, 0.05±0.002 vs. C-ZL, 0.18±0.014; male: C-ZDF, 0.07 ±0.003 vs. C-ZL, 0.18±0.013; $P < 0.01$; Fig. 4B), with greater ratio reduction in females than in males (female C-ZDF, 0.05±0.002 vs. male C-ZDF, 0.07±0.003; $P < 0.05$). Moreover, obese rats exhibited reduced levels of both CaMKKII (female: C-ZDF, 0.34±0.04 vs. C-ZL, 0.62±0.03; male: C-ZDF, 0.75±0.05 vs. C-ZL, 1.04±0.02; $P < 0.05$; Fig. 4C) and P-CaMKKII (female: C-ZDF, 0.002±0.005 vs. C-ZL, 0.11±0.007; male: C-ZDF, 0.01±0.006 vs. C-ZL, 0.18±0.015; $P < 0.01$; Fig. 4D), with also reduced levels of CaMKKII expression in females than males (female C-ZDF, 0.34±0.04 vs. male C-ZDF, 0.75±0.05; $P < 0.05$). In the VL from both sex obese rats, melatonin restored CaMKKII (female, 0.59±0.02; male, 1.13±0.08; $P < 0.05$; Fig. 4C) and P-CaMKKII expression (female, 0.13±0.008; male, 0.12±0.012; $P < 0.01$; Fig. 4D), increasing the P-CaMKKII/CaMKKII ratio (female, 0.21±0.005, $P < 0.01$; male, 0.11 ±0.003, $P < 0.05$; Fig. 4B), and also enhanced CaMKKII and P-CaMKKII levels in both sex lean rats (female, 0.85±0.04; 0.15±0.007; male, 1.23 ±0.03; 0.26±0.017; respectively; $P < 0.05$, Fig. 4C, D). The P-CaMKII/CaMKII ratio was also lower in both sex obese ZDF rats (female, 0.3 ±0.01; male, 0.16±0.01) compared to their respective female (C-ZL, 0.42±0.01; $P < 0.05$) and male (C-ZL, 0.62±0.04; $P < 0.01$) lean control rats (Fig. 4E). Moreover, as shown in Figs. 4F and 4G, CaMKII and P-CaMKII levels, respectively, were also diminished in both sex ZDF rats (female, 0.53±0.02 and 0.17±0.01; male, 0.57±0.13 and 0.11±0.02; respectively) compared to their respective ZL controls (female, 0.87 ±0.03 and 0.36±0.02; male, 1.38±0.23 and 0.85±0.09; respectively, $P < 0.01$). Reduction in the P-CaMKII/CaMKII ratio and P-CaMKII protein expression observed in obese-diabetic rats was greater in males when compared to female rats (female C-ZDF, 0.3±0.01 and 0.17±0.01; vs. male C-ZDF 0.16±0.01 and 0.11±0.02; respectively, $P < 0.05$). After melatonin treatment, protein expression of CaMKII and P-CaMKII was enhanced in the VL from both sex obese (M-ZDF female, 0.86±0.05 and 0.51±0.01; and male, 1.24±0.04 and 0.41±0.03; $P < 0.01$) and also female lean rats (M-ZL CaMKII, 1.16±0.03; $P < 0.05$; and P-CaMKII, 0.67±0.01; $P < 0.01$; Fig. 4F, G respectively), increasing the P-CaMKII/CaMKII ratio in both sex obese (M-ZDF female, 0.67±0.07; and male, 0.41±0.01; $P < 0.01$) and female lean animals (M-ZL, 0.58±0.02; $P < 0.05$; Fig. 4E). Lastly, the P-AMPK/AMPK ratio was observed to be decreased in both sex obese animals (female, 0.46±0.04; and male, 0.46 ±0.03) when compared to ZL control rats (female, 0.77±0.1; and male, 0.77±0.09; $P < 0.01$; Fig. 4H), as well as the AMPK (female C-ZDF, 0.77 ±0.1 vs. C-ZL, 1.31±0.08; and male C-ZDF, 0.7±0.05 vs. C-ZL, 1.32 ±0.04; $P < 0.01$; Fig. 4I) and the P-AMPK levels in the same rats (female C-ZDF, 0.37±0.02 vs. C-ZL, 0.98±0.03; and male C-ZDF, 0.32±0.1 vs. C-ZL, 1.1±0.12; $P < 0.01$; Fig. 4J). As a consequence of the Ca^{2+} thermogenic pathway activation by melatonin, the P-AMPK/AMPK ratio was increased in the VL from both sex obese rats (female, 0.8±0.04; and male, 0.8±0.05; $P < 0.01$; Fig. 4H) due to an increase in the protein expression levels of AMPK and P-AMPK in the VL from the ZDF female (1.39±0.02 and 1.12±0.05, respectively; $P < 0.01$) and male rats (0.89 ±0.09 and 1.03±0.02; $P < 0.05$; Fig. 4I, J respectively). Melatonin effects in the activation of the Ca^{+2}-dependent thermogenic pathway are also shown in blots from Fig. 4K.

3.5. Effects of melatonin on VL thermogenic gene and protein expression

The transcription factor PCG1α serves as a central regulator in the nucleus of thermogenesis, governing the activation of other thermogenic genes such as NRF1 and PPARγ, which contribute significantly to mitochondrial functionality and biogenesis. In both sex obese rats compared to control ZL ones, a decreased PGC1α gene (female, C-ZDF 0.55±0.18 vs. C-ZL 1.11±0.13; male, C-ZDF 0.8±0.03 vs. C-ZL 1.35 ±0.12; $P < 0.05$; Fig. 5A) and protein expression (female, C-ZDF 0.34 ±0.02 vs. C-ZL 0.79±0.01; male, C-ZDF 0.33±0.01 vs. C-ZL 0.73±0.09; $P < 0.01$; Fig. 5B) was observed. Melatonin treated rats, compared to their respective controls, presented increased PCG1α gene expression (female: M-ZDF, 1.02±0.06, $P < 0.05$; and M-ZL, 1.68±0.19, $P < 0.01$;

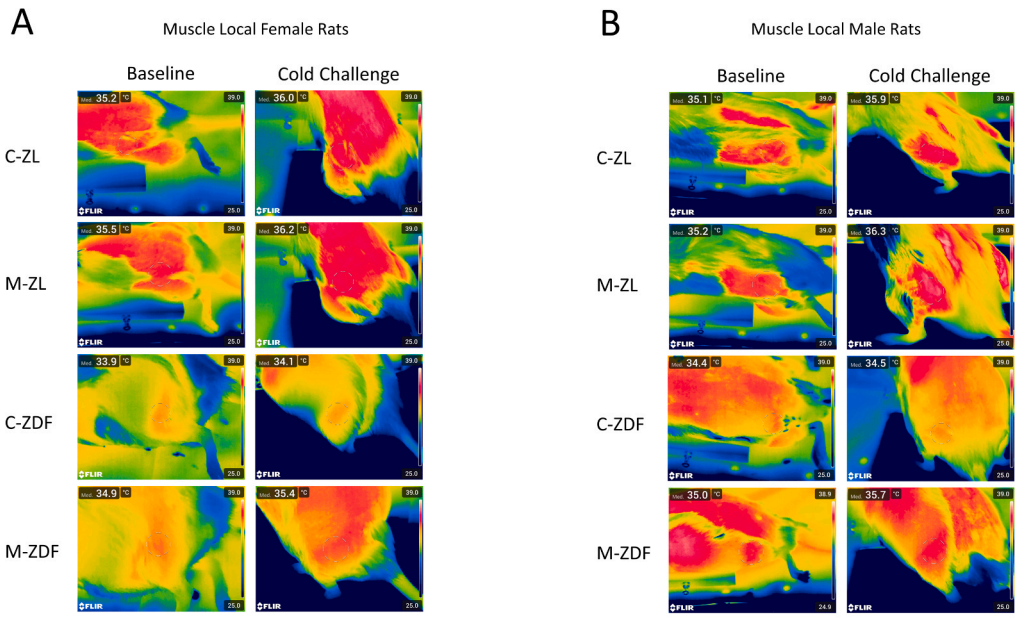

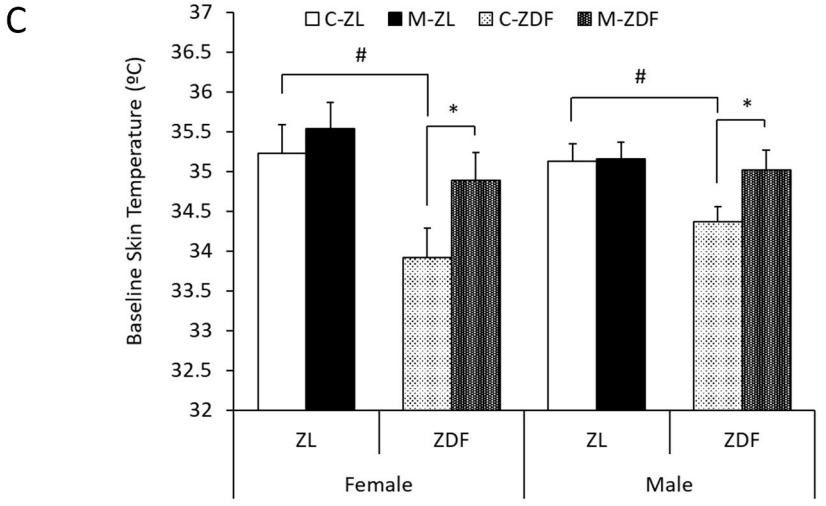

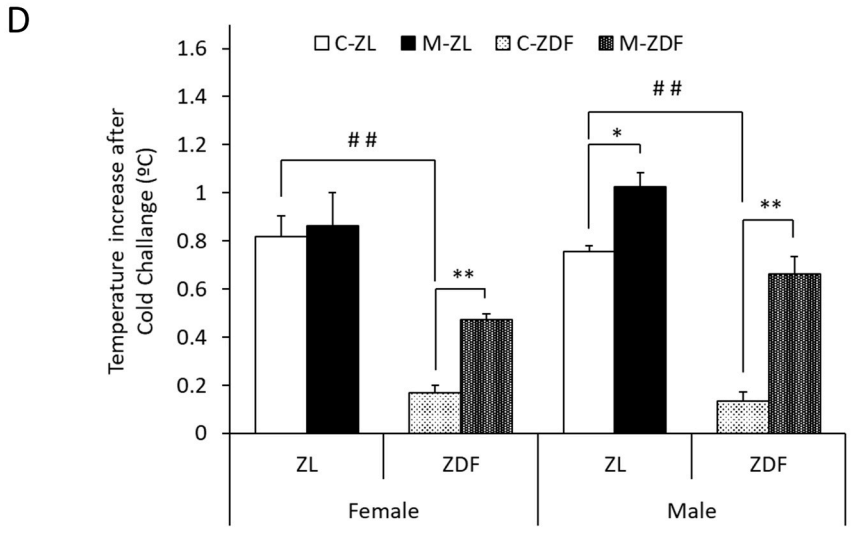

(caption on next page)

Fig. 2. Melatonin effects on Local Superficial Temperature in female and male VL. A-B Representative thermal images of the skin overlying the VL in lean (ZL) and obese (ZDF) rats at thermoneutrality and after cold challenge in female (A) and male (B) animals. The left panel shows basal temperature while the right panel documents the temperature increase after acute cold exposure. C Quantitative Local VL temperature at thermoneutrality. D Quantitative Local VL temperature after cold challenge at 4ºC. Results are expressed as the means ± S.E.M. of 8 animals/group. One-way ANOVA followed by Tukey's post- test was performed for statical analysis (*$P < 0.05$ and **$P < 0.01$ melatonin vs control rats; $^{\#}P < 0.05$ *and* $^{\#\#}P < 0.01$ C-ZDF vs C-ZL rats).

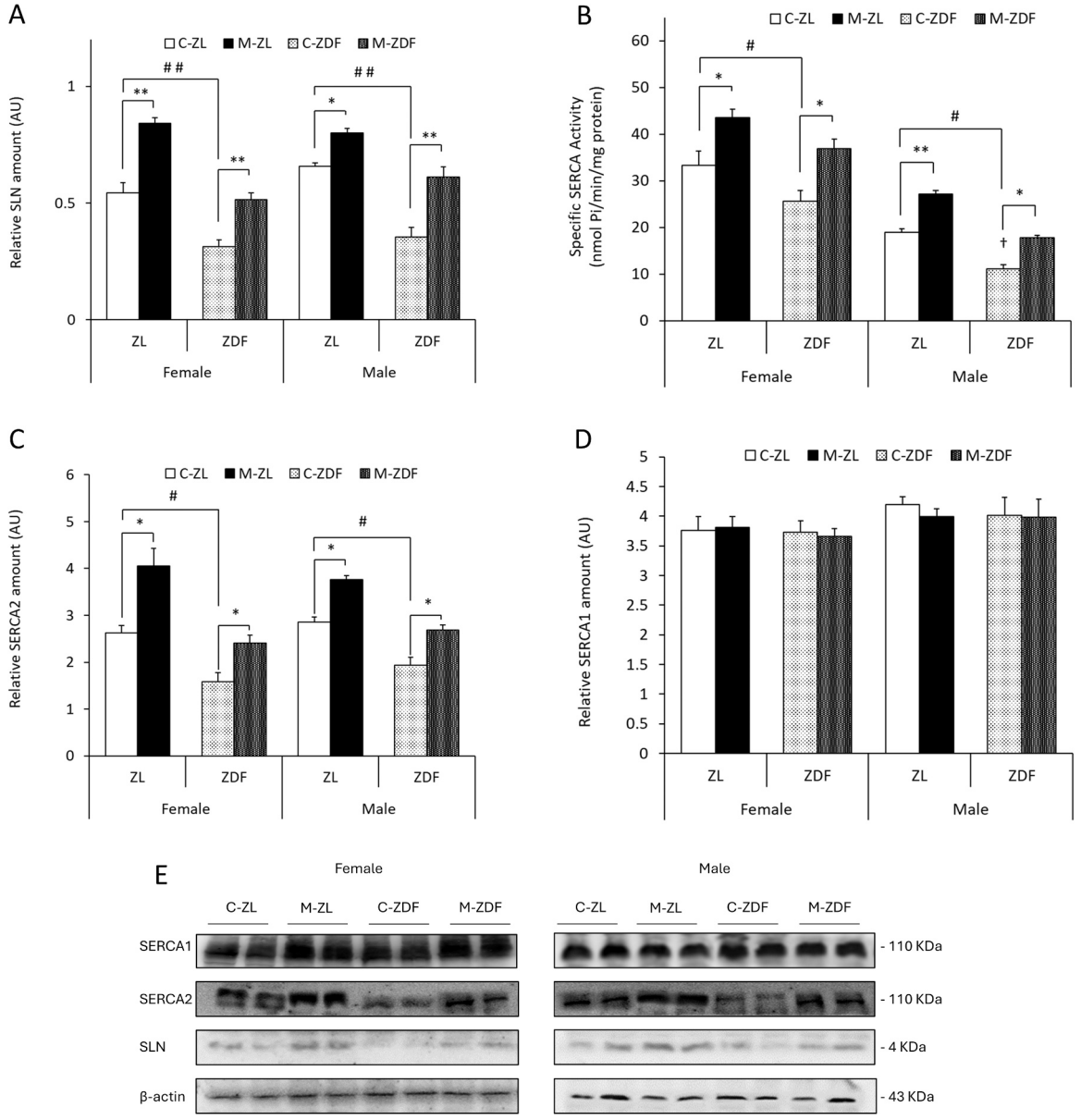

Fig. 3. Melatonin effects on SERCA-SLN uncoupling in female and male VL. A Densitometry quantification of SLN expression in the VL from lean (ZL) and obese (ZDF) rats in female and male animals. **B** Specific SERCA activity in the VL from lean (ZL) and obese (ZDF) rats in female and male animals. **C** Densitometry quantification of SERCA2 expression in the VL from lean (ZL) and obese (ZDF) rats in female and male animals. **D** Densitometry quantification of SERCA1 expression in the VL from lean (ZL) and obese (ZDF) rats in female and male animals. **E** Representative blots of SLN, SERCA2, and SERCA 1 expression in the VL from lean (ZL) and obese (ZDF) rats in female (left) and male (right) animals. Results are expressed as the means ± S.E.M. of three independent experiments in duplicate. One-way ANOVA followed by Tukey's post-test was performed for static analysis (*$P < 0.05$ and **$P < 0.01$ melatonin vs control rats; $^{\#}P < 0.05$ *and* $^{\#\#}P < 0.01$ C-ZDF vs C-ZL rats; †$P < 0.05$ female C-ZDF vs male C-ZDF).

male: M-ZDF, 2.01±0.28, $P < 0.01$; and M-ZL, 1.8±0.22, $P < 0.05$; Fig. 5A), and also, protein expression in VL from both sex obese (female, 0.61±0.06; male, 0.61±0.07; $P < 0.01$) and lean rats (female, 0.91 ±0.03; male, 1.06±0.12; $P < 0.05$; Fig. 5B). Quantitative PCR analysis was performed in the VL muscle of obese animals noticing that increased expression of NRF1 was observed in female compared to male ZDF rats (female, 1.22±0.04; male, 0.26±0.03; $P < 0.01$; Fig. 5C) with no sex-based differences in the other thermogenic gene expression. Melatonin increased the NRF1 gene expression reversing the diminished levels observed in both sex ZDF rats (female, M-ZDF 2.41±0.11 vs. C-ZDF 1.22 ±0.04; $P < 0.01$; male, M-ZDF 0.58±0.06 vs. C-ZDF 0.26±0.03; $P < 0.05$) reaching expression levels of lean counterparts (female, 2.18 ±0.05; $P < 0.01$; male, 0.42±0.04; $P < 0.05$; Fig. 5C). Moreover, PPARγ gene and protein expression was also reduced in VL from both sex ZDF

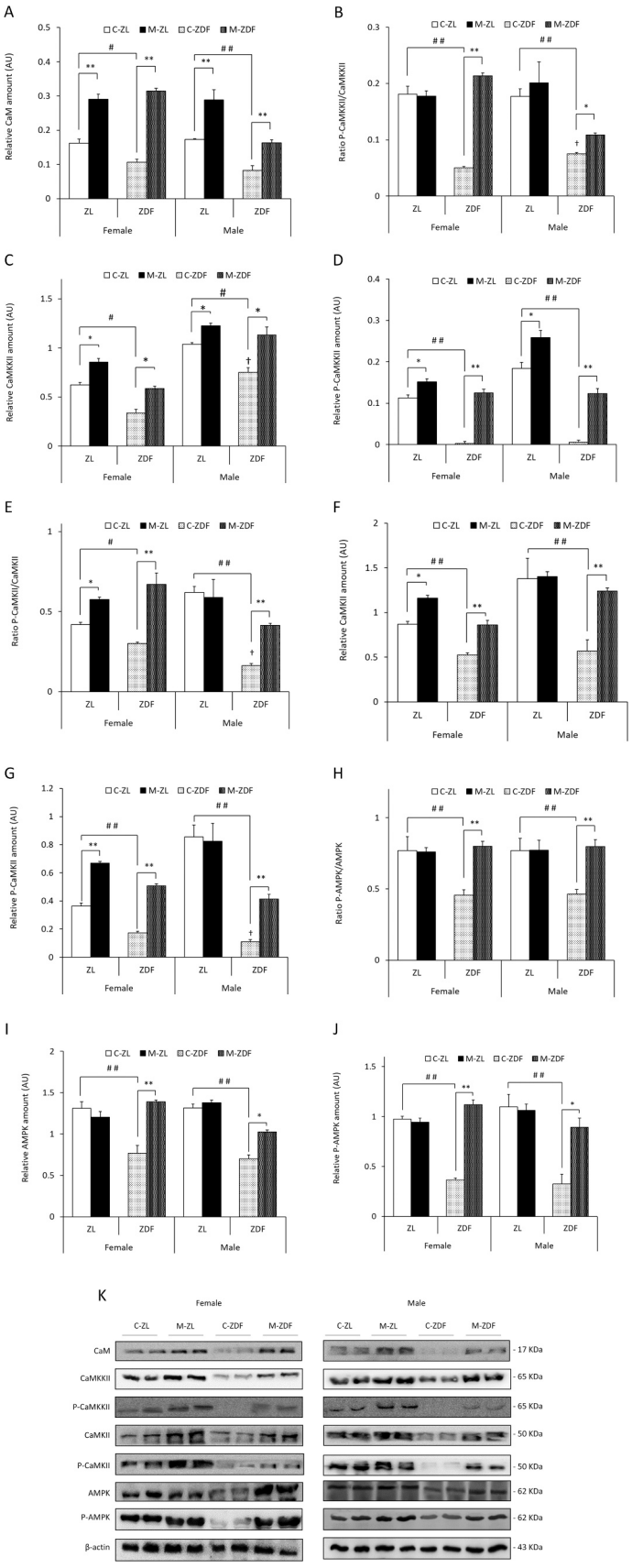

(caption on next page)

Fig. 4. Melatonin effects on the activation of Ca+2-dependent thermogenic pathway in the VL from lean (ZL) and obese (ZDF) rats. A Densitometry quantification of CaM expression in female and male animals. **B** Ratio of P-CaMKKII/CaMKKII expression (activated (phosphorylated)/total) in female and male animals. **C** Densitometry quantification of CaMKKII expression in female and male animals. **D** Densitometry quantification of P-CaMKKII (right) expression in female and male animals. **E** Ratio of P-CaMKII/CaMKII expression (activated (phosphorylated)/total) in female and male animals. **F** Densitometry quantification of CaMKII (left) expression in female and male animals. **G** Densitometry quantification of P-CaMKII (right) expression in female and male animals. **H** Ratio of P-AMPK/AMPK expression (activated (phosphorylated)/total) in female and male animals. **I** Densitometry quantification of AMPK expression in female and male animals. **J** Densitometry quantification of P-AMPK (right) expression in female and male animals. **K** Representative blots of CaM, CaMKKII, P-CaMKKII, CaMKII, P-CaMKII, AMPK, and P-AMPK expression in the VL from lean (ZL) and obese (ZDF) rats in female (left) and male (right) animals. Results are expressed as the means ± S.E.M. of three independent experiments in duplicate. One-way ANOVA followed by Tukey's post-test was performed for static analysis (*$P < 0.05$ and **$P < 0.01$ melatonin vs control rats; $^{\#}P < 0.05$ *and* $^{\#\#}P < 0.01$ C-ZDF vs C-ZL rats; †$P < 0.05$ female C-ZDF vs male C-ZDF).

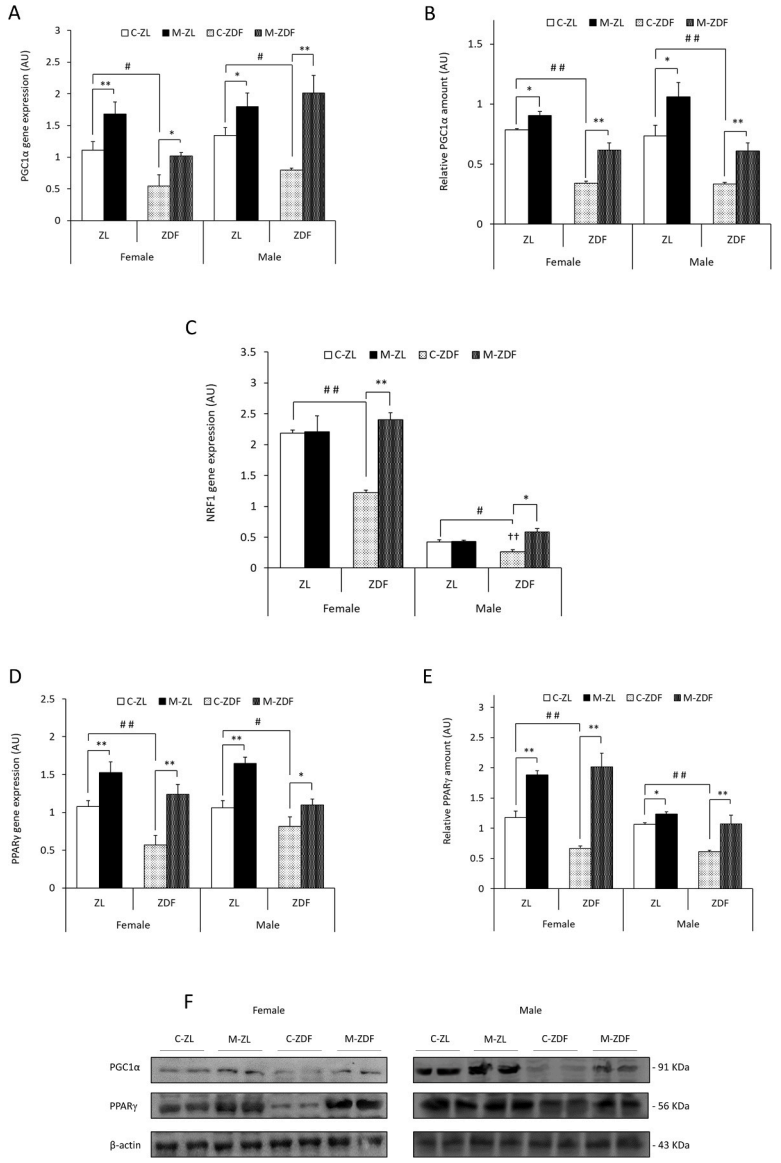

Fig. 5. Melatonin effects on thermogenic gene and protein expression in female and male VL. A Relative PGC1α gene expression (mRNA levels quantification) in the VL from lean (ZL) and obese (ZDF) animals. **B** Densitometry quantification of PGC1α expression in the VL from lean (ZL) and obese (ZDF) animals. **C** Relative NRF1 gene expression (mRNA levels quantification) in the VL from lean (ZL) and obese (ZDF) animals. **D** Relative PPARγ gene expression (mRNA levels quantification) in the VL from lean (ZL) and obese (ZDF) animals. **E** Densitometry quantification of PPARγ expression in the VL from lean (ZL) and obese (ZDF) animals. **F** Representative blots of PGC1α and PPARγ protein expression in the VL from lean (ZL) and obese (ZDF) animals. Results are expressed as the means ± S.E.M. of three independent experiments in triplicate (gene expression) or duplicate (protein expression). One-way ANOVA followed by Tukey's post-test was performed for static analysis (*$P < 0.05$ and **$P < 0.01$ melatonin vs control rats; $^{\#}P < 0.05$, *and* $^{\#\#}P < 0.01$ C-ZDF vs C-ZL rats; †$P < 0.05$ and ††$P < 0.01$ female C-ZDF vs male C-ZDF).

rats (female, 0.57±0.12 and 0.67±0.04; and male, 0.82±0.13 and 0.61 ±0.02, respectively) compared to their ZL control female (PPARγ gene and protein expression respectively: 1.07±0.08 and 1.18±0.11; $P < 0.01$) and male (PPARγ gene expression 1.06±0.09, $P < 0.05$; PPARγ protein expression 1.06±0.03, $P < 0.01$) animals (Fig. 5D, E). After melatonin treatment, the PPARγ gene and protein expression of the VL muscle was raised in all phenotype female rats (M-ZDF gene, 1.24±0.13, and protein expression, 2.01±0.23; M-ZL gene, 1.53±0.14, and protein

expression, 1.88±0.06; $P < 0.01$). Melatonin also increased male obese and lean PPARγ gene (M-ZDF, 1.1±0.08; $P < 0.05$; M-ZL, 1.64±0.09; $P < 0.01$) and protein expression (M-ZDF, 1.07±0.14; $P < 0.01$; M-ZL, 1.24±0.03; $P < 0.05$) in the VL muscle (Fig. 5D, E). The effect of melatonin on increasing thermogenic protein expression is also shown in blots from Fig. 5F.

3.6. Effects of melatonin on VL mitochondrial biogenesis

Given the pivotal role of mitochondrial functionality in SKM energy metabolism and the established connection between mitochondrial biogenesis and thermogenesis, we explored the impact of melatonin treatment on mitochondriogenesis. This was accomplished by measuring mtDNA copy number and the activity of CS, the rate-limiting enzyme in the tricarboxylic acid cycle within the matrix of mitochondria, in isolated mitochondria from the VL muscle of both sex and phenotype animals. The CS activity was quantified as nmol/min/mg protein. Both sex C-ZDF rats were found to present decreased mitochondriogenesis by reduced relative mtDNA copy number (female, 0.21 ±0.09; male, 0.27±0.06; $P < 0.05$; Fig. 6A) and CS activity (female, 6.08 ±0.11; male, 6.25±0.17; $P < 0.01$; Fig. 6B) compared to lean littermates (relative mtDNA copy number and CS activity respectively, female 0.69 ±0.1 and 9.39±0.2; male, 1.01±0.27 and 10.06±0.12). Chronic melatonin treatment resulted in an increase in relative mtDNA copy number in both phenotype female (M-ZL, 1.83±0.07; M-ZDF, 2.5±0.15; $P < 0.01$) and male (M-ZL, 2.64±0.1; M-ZDF, 1.63±0.27; $P < 0.01$) animals (Fig. 6A). Also, CS activity was enhanced after melatonin treatment in VL from both sex lean (female, 10.95±0.21; male, 11.86±0.21; $P < 0.05$) and obese rats (female, 10.09±0.26, $P < 0.01$; male, 8.03±0.22, $P < 0.05$; Fig. 6B).

4. DISCUSSION

In previous studies, we explored the antiobesity and metabolic regulator effect of acute administration of melatonin in young male ZDF rats, demonstrating that melatonin has been shown to restrain obesity and improve metabolic function [31,46,47] in part through activation of brown and browning of subcutaneous body fat [32,48–51]. In the present study, we have shown that chronic administration of melatonin to adult female and male ZDF rats also improved obesity by inducing uncoupling of SKM SERCA-SLN mediated by CaMKII/AMPK/PGC1α pathway and mitochondrial biogenesis, and then thermogenic capacity. While no significant differences in initial body weight between all groups were found, higher final BW and greater BW gain of both sex ZDF have been recorded and agreed with those previous reports obtained at a similar age in this strain of male rats [52] and female [53] group compared to ZL animal. Furthermore, male ZDF rats were found to have a higher final BW as a consequence of an increased body weight gain compared to female ZDF animals. These data are consistent with previous report in the same rat strain at a similar age where male ZDF rats presented greater body weight compared to female ones [54–57]. In addition, increased total and mesenteric visceral fat index of the female ZDF group compared to male ZDF animals observed in the present study is consistent with previous reports obtained at a similar age in obese rodents [58] and humans [59,60], supporting the idea that the female sex, from a translational perspective, is a risk factor for human obesity and comorbidities development [61,62] even though women are more resistant to weight gain than men. To our knowledge, this is the first demonstration that chronic melatonin administration can reduce obesity in adult female and male ZDF rats, by limiting BW gain and BMI, by 17% in obese female and male rats, and by 14% in male lean ones without affecting the food intake. As expected, even more than that acute-treatment study showed a 12% reduction in young male obese rats [31]. At the same time, melatonin reduces such obesity by decreasing the relative visceral adiposity, the main pro-obese white adipose tissue that is strongly related to metabolic alterations, in adult female and male obese and lean rats. Previous reports of this melatonin effect have been studied in different male, middle-aged rat models [63–65] or young Sprague–Dawley lean rats [66], and with diet-induced obesity [67]. It was also observed that melatonin treatment reduces the rodents' male-relative visceral obesity, concerning both retroperitoneal and epididymal, or central fat depots, which are linked to glucose intolerance and insulin resistance [64,65,68]. SKM, as a principal metabolic consumer, determines systemic energy homeostasis [69]. Perturbation of the SKM metabolism elevates the risk of a variety of diseases including obesity and its metabolic disorders [70]. Recently, we showed that relative VL weight was significantly lower in male obese ZDF than its mate lean rat [33] which reflects the SKM loss function characteristic in obesity [71], and melatonin treatment was found to restore it completely [33].

Furthermore, in the present work, we demonstrated that melatonin treatment increased the thermogenic activity of VL as indicated by a temperature rise of its local skin recorded by the thermal camera which may explain the reduction of final BW and central adiposity in obese rats through a mechanism for a potential switch of energy resource into fat oxidation and an upregulation of adaptive thermogenesis by SKM NST. In this respect, we recently showed that melatonin increased the oxidative capacity of VL from male obese ZDF rats [33], although the effect on VL mitochondrial oxidative metabolism of this indolamine is still unclear and needs to be elucidated. SKM NST, together with the

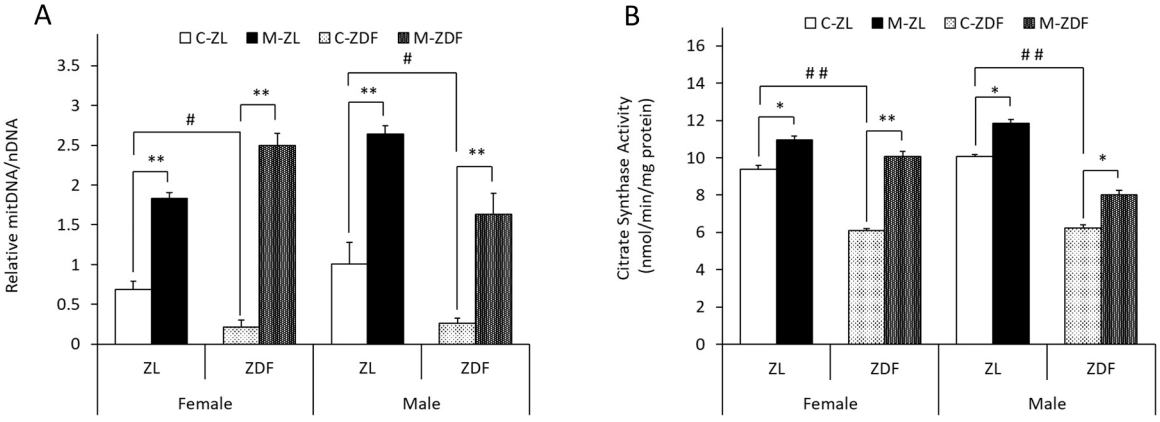

Fig. 6. Melatonin effects on mitochondrial biogenesis in female and male VL. A Relative quantification of the mtDNA copy number by measuring the ratio of mitochondrial and nuclear DNA in the VL from lean (ZL) and obese (ZDF) rats. **B** CS activity in isolated mitochondria from the VL from lean (ZL) and obese (ZDF) rats. Results are expressed as the means ± S.E.M. of three independent experiments in triplicate. One-way ANOVA followed by Tukey's post-test was performed for static analysis (*$P < 0.05$ and **$P < 0.01$ melatonin vs control rats; $^{\#}P < 0.05$, and $^{\#\#}P < 0{\cdot}01$ C-ZDF vs C-ZL rats).

activation of both thermogenic adipose tissues observed in the same rat model in our previous studies [32,51] provides an explanation for melatonin control obesity animals, in the absence of significant changes in locomotor activity and food intake. Moreover, melatonin treatment sensitizes VL to the thermogenic effect of acute cold exposure in both lean and obese rats, as demonstrated by the rise of the skin temperature of the VL region, detected by the thermal camera. Collectively, the above data demonstrated that chronic melatonin administration activates VL thermal function in obese and lean in both sex rats. These results are coherent with data obtained in previous studies on the same male-rat strain, where melatonin was shown to increase also the local inguinal and scapular skin temperature through an increased beige and BAT UCP1 expression [32,49,51]. It is well known that adrenergic activation by a variety of physiological stimuli including cold exposure leads to the browning of WAT [72,73] and activation of BAT [74] inducing UCP1 expression, as well as enhanced SKM NST inducing SERCA-SLN uncoupling [5].

SLN modulates SERCA activity by uncoupling ATP hydrolysis in this pump [75] and generating an increase in heat production [76] thereby playing an important role in animal thermoregulation [3]. In humans, obesity is related to decreased NST and resistance to loss of fat [77]. In addition, SLN KO mice diminish adaptive SKM thermogenesis, increase BW gain, and decrease fat oxidation [3]. In this sense, the present results show that SLN expression was 2-fold lower in VL of both female and male ZDF rats compared to its correspondent lean controls. Moreover, SERCA activity and protein expression were decreased in both female and male obese ZDF than its correspondent ZL rat, which agrees with another study that shows that diet-induced obesity lowered SERCA-2a expression and activity [78]. In the present study, we describe for the first time that SERCA activity was also lower in VL muscle from male ZDF compared to female ZDF rats. This data is coherent with the decreased τCa, the inverse measurement of SERCA activity, found in the cardiac muscle from female endotoxemic mice compared to male ones [79] and the reduced ATPase activity observed in response to Ca^{2+} in the heart of male adult rats compared to female ones [80], highlighting the importance of chronic low-grade inflammation in the physiopathology of both obesity and sepsis and the tight relationship between them [81]. Being SLN a regulator of SERCA activity and the molecular effector of SKM NST, in this study, we also demonstrate a novel finding that both sex melatonin-treated obese and lean animals exhibited an increased VL NST by increasing SLN protein levels, SERCA activity, and SERCA2 protein expression recovering the loss of expression showed in obese animals with no effects on SERCA1 protein expression. The cold adaptation increases specifically SERCA2-SLN uncoupling (Pant et al., 2015), and SLN overexpression was shown to promote mitochondrial biogenesis and oxidative metabolism in mice [8] increasing SKM NST and limiting central obesity, being these results coherent with those obtained in this study. Furthermore, SERCA-SLN uncoupling modulates intracellular Ca^{2+} signaling pathways, fostering mitochondrial biogenesis and oxidative metabolism being this adaptation crucial to fulfilling elevated energy requirements in muscle tissue [83].

In addition, they demonstrated that SERCA-SLN uncoupling affects cytosolic Ca^{2+} transit and activates the CamKII/PGC-1α axis to increase mitochondrial biogenesis and oxidative metabolism in mice [8]. Obesity is also closely related to the dysregulation of SKM Ca^{2+} management [84] which may be explained by a decreased activation of Ca^{2+} signaling pathways. Results obtained in the present work show for the first time that obese and diabetic ZDF rats present lower activation of CaM/-CaMKKII/CaMKII/AMPK molecular pathway decreasing the expression and/or the phosphorylation of these proteins compared to lean ZL ones. All these data are in accordance with new studies in diet-induced obese mice in both sexes showed reduced activation of SKM AMPK, the master regulator of cellular metabolism and mitochondrial homeostasis [85], by reduced phosphorylation of Ca^{2+}-dependent regulatory proteins such as CaMKII and CaMKKII [86,87], even altering the SKM CaMKK/AMPK pathway in both sex offspring of obese mothers [87]. In addition, mice with insulin resistance present reduced expression of phosphorylated active forms of AMPK and CaMK [88]. Moreover, in the liver of obese diabetic mice, another insulin-sensitive organ, CaM expression was reduced attenuating hyperglycemia observed in animal models of diabesity [89]. In the same way, Ca^{2+} dysregulation by SLN deficiency in mice improves obesity and reduces the CaMKII activation pathway [8]. In the present work, we also show for the first time that female obese-diabetic ZDF rats present an increased ratio of P-CaMKII/CaMKII, while male ZDF rats exhibit increased levels of activated CaMKKII, emphasizing the sex-related differences in the pathway activation for intracellular Ca^{2+} homeostasis regulation in the VL muscle from these animals. These data are consistent with the findings reported in mice with pressure overload-induced cardiac hypertrophy and heart failure, as remarkable alterations in the heart from obese subjects [90], and where female animals were found to present higher levels of the activated form of CaMKII than male ones [91]. These differences in Ca^{2+} handling were also observed in healthy rodents' hearts [92] and brains, where animals were shown to activate different and sex-specific pathways for Ca^{2+} regulation in distinct cellular processes, being male rodents more related to CaMKKII and PKA activation, and female ones with CaMKII [93,94]. Furthermore, it is widely recognized that SKM and heart from female rodents and humans present more sensitivity to Ca^{2+} flux variations and better intracellular and intramitochondrial Ca^{2+} handling [92,95–97] possibly due to the increased activation of CaMKII observed in the present study supporting the widely extended idea that female animals are protected against diabesity and its complications. Given that CaMKII is essential for muscle contraction, intracellular Ca^{2+} homeostasis, and glucose control in the progression of T2DM [98], the increased P-CamKII levels observed in female ZDF rats suggest a potential protective mechanism against diabesity progression and associated comorbidities. Meanwhile, in male counterparts, it appears that compensatory mechanisms, such as heightened activation of CaMKKII, might be active, leading both female and male mechanisms to the activation of effector proteins such as AMPK and PGC1α which regulated mitochondriogenesis [20]. CaMKII activation is mediated by CaM when it binds to free Ca^{2+} in the cytosol [99], and/or CaMKKII, a potent regulator of whole-body energy homeostasis [100], leading this activation to a higher AMPK phosphorylation, and fatty acid mobilization and oxidation in the SKM [21]. Further research is warranted to elucidate the precise molecular mechanisms regulating this sex-specific Ca^{2+} pathway activation, intraorganellar Ca^{2+} transport in SKM, their implications in therapeutic interventions, and the role of melatonin in this matter.

As mentioned before, in the present study we reported that melatonin was found to increase SERCA2-SLN uncoupling leading to a higher expression of SKM CaM in both sex and phenotype animals, and activation of CaMKKII/CaMKII/AMPK thermogenic molecular pathway inducing higher rates of phosphorylated active form of these proteins in VL from both sex obese and diabetic ZDF rats, limiting diabesity. Melatonin coincubation in rat myoblast culture was shown to improve de activation of CaMKII [101] also activating the AMPK pathway in SKM from lean-treated Wistar rats [102]. Furthermore, melatonin activation of SKM AMPK by its phosphorylation was also related to reduced body weight gain in diet-induced obese mice [103]. Moreover, physiological stimuli like cold and exercise increased SLN expression, being this process related to increased activation of Ca^{2+}-dependent thermogenic pathways inducing CaMKKII, CaMKII, and AMPK phosphorylation in SKM from both sex lean and obese rodents [82,87,102,104]. Other stimuli such as hindlimb cast immobilization of mice were also found to increase SKM NST by inducing SLN expression and CaMKII activation [105], showing the close relationship between SERCA-SLN uncoupling in SKM NST and Ca^{2+}-dependent thermogenic pathway activation.

VL extracts analysis also demonstrated that VL areas expressed lower gene and protein amounts of PGC1α, NRF1, and PPARγ in both sex-obese rats. These results are coherent with data obtained in previous studies where PGC1α, NRF1, and PPARγ protein and/or gene expression were

decreased in SKM from obese mice [106–108]. Interestingly, NRF1 gene expression was strongly higher in the VL from female rats compared to male ones. This may suggest that VL from female rats is more oxidative than VL muscle from males, being consistent with data obtained in other rodents and humans where oxidative slow-twitch type I fibers were found to be increased and/or glycolytic fast-twitch type IIb fibers diminished in female compared to males [109]. Moreover, these type I fibers were not associated with an increase in PGC1α and mitochondriogenesis, which are linked to AMPK activation [110], but with an increase in CaMK activation [111] as reported in this study, where an increased CaMKII ratio and NRF1 was observed in female compared to male rats with no sex-related differences in AMPK ratio, PGC1α expression and mitochondriogenesis in ZDF rats. This NRF1 expression sexual dimorphism was also observed in other insulin-sensitive organs, like the liver, in mice maintained with a hypercaloric diet [112]. Further analysis of fiber type composition and oxidative capacity in VL from male and female ZDF rats will help in the understanding of these sex-related differences. Also, here we prove for the first time that melatonin treatment recovered PGC1α, NRF1, and PPARγ VL deficient protein and/or gene expression in obese-diabetic conditions, being highly related with better MB, mitochondrial function, and thermogenesis, as showed in both sexes ZDF and ZL treated rats. Previous studies showed that melatonin increases SKM PGC1α and NRF1 expression in rats curbing insulin resistance, the first step of obesity, produced after palmitic acid-induced lipotoxicity [101], and in rats with T2DM [113]. Moreover, in humans, melatonin increases PPARγ gene expression reducing insulin resistance in women with polycystic ovary syndrome [114]. On one hand, a recent study showed that melatonin enhances the type II fast fibers in a glycolytic SKM by reducing PPARγ expression in weaned piglets [115]. On the other hand, we reported that melatonin treatment improves the oxidative capacity of VL, a mixed fiber type SKM, in male ZDF rats [33] being coherent with PPARγ higher expression levels obtained in this work. This highlights the key role of melatonin as a metabolic regulator according to the fiber type composition of each SKM.

Many studies reported defects in SKM mitochondrial dynamics and function in obesity affecting mitochondrial content, including decreased mitochondrial gene and protein expression, and lower activity of CS (a marker of mitochondrial content) [116]. Furthermore, CS activity of SKM in young female obese ZDF rats was lower compared to its lean control rats [117]. All these data are consistent with results obtained in the present work in which obesity was found to reduce VL CS activity and mtDNA copy number in both sexes of adult ZDF rats. Additionally, our results revealed that melatonin administration led to a significant augmentation in the CS activity and mtDNA copy number in VL from both sex and phenotype animals. Other results indicating that melatonin increases the mitochondriogenesis of SKM in sedentary Wistar rats [102], are in harmony with our prior findings in other insulin-sensitive organs such as the liver [118] or in other thermogenic tissues such as BAT in the same rat strain [51], and is consistent with increased VL thermogenic activity observed after melatonin treatment in the present study. Ultimately, the rise in energy dissipation results in improved dysmetabolic features in these rodents, thereby, further studies in mixed fiber type SKM mitochondrial function and oxidative metabolism are needed for a better understanding of the melatonin role in SKM metabolic plasticity control.

5. Conclusion

Taken together, our findings suggest targeting the thermogenesis effects of chronic melatonin treatment on SERCA2-SLN uncoupling and mitochondrial biogenesis in the SKM of female and male ZDF rats, with the browning effect of WAT and the activation of BAT seen in this rat model in our earlier studies, in the absence of significant changes in locomotor activity and food intake [31,32,51], melatonin is presented as a promising therapeutic approach for mitigating human obesity and metabolic syndrome. Furthermore, we have demonstrated that melatonin sensitizes SKM cells to other thermogenic stimuli, such as cold, it is presumed that it can potentiate the thermogenic effect of exercise. Further validation studies in other models, other melatonergic agents, and humans will be not only necessary to confirm our results but also aimed at determining the optimal high dosage, which we estimate the effective dose used in this study to humans based on the calculation of the human equivalent dose to be between 12 and 120 mg/day orally for a 75 kg adult individual. Also, we aimed at determining the right hour of the day, course time, and best via to administrate melatonin to increase energy expenditure in humans.

Funding

This study was supported by grant PID2021-125900OB-I00 funded by MCIN/AEI/10.13039/501100011033 and, as appropriate, by “ERDF A way of making Europe”, by the “European Union” or by the “European Union NextGenerationEU/PRTR”.

Ethical statement

The study was conducted according to the guidelines of the Declaration of Helsinki and approved by the Ethical Committee of the University of Granada (Granada, Spain) according to the European Union guidelines. The protocol code is 23/06/2021/096-CEEA.

Declaration of Competing Interest

The authors declare that they have no known competing financial interests or personal relationships that could have appeared to influence the work reported in this paper.

Acknowledgements

The authors thank Antonio Tirado and Vanessa Blanca for their technical assistance.

Appendix A. Supporting information

Supplementary data associated with this article can be found in the online version at doi:10.1016/j.biopha.2024.116314.

References

[1] B. Sahu, S. Pani, G. Swalsingh, N.C. Bal, Epigenetic mechanisms in regulation of adaptive thermogenesis in skeletal muscle, Front. Endocrinol. *10* (2019) 517.
[2] N.C. Bal, M. Periasamy, Uncoupling of sarcoendoplasmic reticulum calcium atpase pump activity by sarcolipin as the basis for muscle non-shivering thermogenesis, Philos. Trans. R. Soc. B: Biol. Sci. *375* (2020).
[3] N.C. Bal, S.K. Maurya, D.H. Sopariwala, S.K. Sahoo, S.C. Gupta, S.A. Shaikh, M. Pant, L.A. Rowland, S.A. Goonasekera, J.D. Molkentin, et al., Sarcolipin is a newly identified regulator of muscle-based thermogenesis in mammals, Nat. Med. *18* (2012) 1575–1579, https://doi.org/10.1038/nm.2897.
[4] J.P. Fuller-Jackson, B.A. Henry, Adipose and skeletal muscle thermogenesis: studies from large animals, J. Endocrinol. *237* (2018) R99–R115.
[5] H. Li, C. Wang, L. Li, L. Li, Skeletal muscle non-shivering thermogenesis as an attractive strategy to combat obesity, Life Sci. *269* (2021) 119024.
[6] B.F. Palmer, D.J. Clegg, Non-shivering thermogenesis as a mechanism to facilitate sustainable weight loss, Obes. Rev. *18* (2017) 819–831.
[7] M. Pant, N.C. Bal, M. Periasamy, Sarcolipin: a key thermogenic and metabolic regulator in skeletal muscle, Trends Endocrinol. Metab. *27* (2016) 881–892.
[8] S.K. Maurya, J.L. Herrera, S.K. Sahoo, F.C.G. Reis, R.B. Vega, D.P. Kelly, M. Periasamy, Sarcolipin signaling promotes mitochondrial biogenesis and oxidative metabolism in skeletal muscle, Cell Rep. *24* (2018) 2919–2931, https://doi.org/10.1016/j.celrep.2018.08.036.
[9] P. Puigserver, B.M. Spiegelman, Peroxisome proliferator-activated receptor-γ coactivator 1α (PGC-1α): transcriptional coactivator and metabolic regulator, Endocr. Rev. *24* (2003) 78–90.
[10] C. Handschin, B.M. Spiegelman, The role of exercise and PGC1α in inflammation and chronic disease, Nature *454* (2008) 463–469.
[11] H. Crossland, D. Constantin-Teodosiu, P.L. Greenhaff, The regulatory roles of ppars in skeletal muscle fuel metabolism and inflammation: impact of ppar

agonism on muscle in chronic disease, contraction and sepsis, Int. J. Mol. Sci. *22* (2021) 9775, https://doi.org/10.3390/ijms22189775.
[12] J.E. Dominy, P. Puigserver, Mitochondrial biogenesis through activation of nuclear signaling proteins, Cold Spring Harb. Perspect. Biol. *5* (2013) a015008, https://doi.org/10.1101/cshperspect.a015008.
[13] S.R. Costford, E.L. Seifert, V. Bézaire, M.F. Gerrits, L. Bevilacqua, A. Gowing, M. E. Harper, The Energetic Implications of Uncoupling Protein-3 in Skeletal Muscle, Appl. Physiol. Nutr. Metab. *32* (2007) 884–894.
[14] R.C. Scarpulla, Metabolic control of mitochondrial biogenesis through the PGC-1 family regulatory network, Biochim. Biophys. Acta Mol. Cell. Res. *1813* (2011) 1269–1278.
[15] V.A. Convertino, E.R. Morey, J.E. Greenleaf, Reduction in plasma calcium during exercise in man, Nature *299* (1982) 658.
[16] N. Chhimpa, N. Singh, N. Puri, H.P. Kayath, The novel role of mitochondrial citrate synthase and citrate in the pathophysiology of Alzheimer's disease, J. Alzheimer's Dis. *94* (2023) S453–S472.
[17] W.W. Winder, B.F. Holmes, D.S. Rubink, E.B. Jensen, M. Chen, J.O. Holloszy, Activation of AMP-activated protein kinase increases mitochondrial enzymes in skeletal muscle, J. Appl. Physiol. *88* (2000) 2219–2226, https://doi.org/10.1152/jappl.2000.88.6.2219.
[18] D.G. Hardie, F.A. Ross, S.A. Hawley, AMPK: a nutrient and energy sensor that maintains energy homeostasis, Nat. Rev. Mol. Cell Biol. *13* (2012) 251–262.
[19] G.R. Steinberg, B.E. Kemp, AMPK in health and disease, Physiol. Rev. *89* (2009) 1025–1078.
[20] M. Iwabu, T. Yamauchi, M. Okada-Iwabu, K. Sato, T. Nakagawa, M. Funata, M. Yamaguchi, S. Namiki, R. Nakayama, M. Tabata, et al., Adiponectin and adipoR1 regulate PGC-1α and mitochondria by Ca 2+ and AMPK/SIRT1, Nature *464* (2010) 1313–1319, https://doi.org/10.1038/nature08991.
[21] M.A. Raney, L.P. Turcotte, Evidence for the involvement of CaMKII and AMPK in Ca2+- dependent signaling pathways regulating FA Uptake and oxidation in contracting rodent muscle, J. Appl. Physiol. *104* (2008) 1366–1373, https://doi.org/10.1152/japplphysiol.01282.2007.
[22] J. Tallis, R.S. James, F. Seebacher, The effects of obesity on skeletal muscle contractile function, J. Exp. Biol. *221* (2018) jeb163840.
[23] M. Periasamy, J.L. Herrera, F.C.G. Reis, Skeletal muscle thermogenesis and its role in whole body energy metabolism, Diabetes Metab. J. *41* (2017) 327–336.
[24] M. Periasamy, S.K. Maurya, S.K. Sahoo, S. Singh, F.C.G. Reis, N.C. Bal, Role of SERCA pump in muscle thermogenesis and metabolism, Compr. Physiol. *7* (2017) 879–890, https://doi.org/10.1002/cphy.c160030.
[25] M.L. Bonet, P. Oliver, A. Palou, Pharmacological and nutritional agents promoting browning of white adipose tissue, Biochim. Biophys. Acta Mol. Cell Biol. Lipids *1831* (2013) 969–985.
[26] R.J. Wurtman, J. Axelrod, L.S. Phillips, Melatonin synthesis in the pineal gland: control by light, Science *142* (1963) 1071–1073, https://doi.org/10.1126/science.142.3595.1071.
[27] J. Stefulj, M. Hörtner, M. Ghosh, K. Schauenstein, I. Rinner, A. Wölfler, J. Semmler, P.M. Liebmann, Gene expression of the key enzymes of melatonin synthesis in extrapineal tissues of the rat, J. Pineal Res *30* (2001) 243–247, https://doi.org/10.1034/j.1600-079X.2001.300408.x.
[28] G. Cheng, T. Ma, Z. Deng, G. Gutiérrez-Gamboa, Q. Ge, P. Xu, Q. Zhang, J. Zhang, J. Meng, R.J. Reiter, et al., Plant-derived melatonin from food: a gift of nature, Food Funct. *12* (2021) 2829–2849.
[29] B. Salehi, F. Sharopov, P.V.T. Fokou, A. Kobylinska, L. de Jonge, K. Tadio, J. Sharifi-Rad, M.M. Posmyk, M. Martorell, N. Martins, et al., Melatonin in medicinal and food plants: occurrence, bioavailability, and health potential for humans, Cells *8* (2019) 681.
[30] M.A. Raskind, B.L. Burke, N.J. Crites, A.M. Tapp, D.D. Rasmussen, Olanzapine-induced weight gain and increased visceral adiposity is blocked by melatonin replacement therapy in rats, Neuropsychopharmacology *32* (2007) 284–288, https://doi.org/10.1038/sj.npp.1301093.
[31] A. Agil, M. Navarro-Alarcõn, R. Ruiz, S. Abuhamadah, M.Y. El-Mir, G.F. Vázquez, Beneficial effects of melatonin on obesity and lipid profile in young zucker diabetic fatty rats, J. Pineal Res. *50* (2011) 207–212, https://doi.org/10.1111/j.1600-079X.2010.00830.x.
[32] A. Jiménez-Aranda, G. Fernández-Vázquez, D. Campos, M. Tassi, L. Velasco-Perez, D.X. Tan, R.J. Reiter, A. Agil, Melatonin induces browning of inguinal white adipose tissue in zucker diabetic fatty rats, J. Pineal Res. *55* (2013) 416–423, https://doi.org/10.1111/jpi.12089.
[33] D. Salagre, E. Raya Álvarez, C.M. Cendan, S. Aouichat, A. Agil, Melatonin improves skeletal muscle structure and oxidative phenotype by regulating mitochondrial dynamics and autophagy in zücker diabetic fatty rat, Antioxidants *12* (2023) 149, https://doi.org/10.3390/antiox12081499.
[34] A. Agil, E.K. Elmahallawy, J.M. Rodríguez-Ferrer, A. Adem, S.M. Bastaki, I. Al-Abbadi, Y.A. Fino Solano, M. Navarro-Alarcón, Melatonin increases intracellular calcium in the liver, muscle, white adipose tissues and pancreas of diabetic obese rats, Food Funct. *6* (2015) 2671–2678, https://doi.org/10.1039/c5fo00590f.
[35] H.M. Yeung, M.W. Hung, M.L. Fung, Melatonin ameliorates calcium homeostasis in myocardial and ischemia-reperfusion injury in chronically hypoxic rats, J. Pineal Res. *45* (2008) 373–382, https://doi.org/10.1111/j.1600-079X.2008.00601.x.
[36] J. Siwy, C. Zoja, J. Klein, A. Benigni, W. Mullen, B. Mayer, H. Mischak, J. Jankowski, R. Stevens, A. Vlahou, et al., Evaluation of the zucker diabetic fatty (ZDF) rat as a model for human disease based on urinary peptidomic profiles, PLoS One *7* (2012) e51334, https://doi.org/10.1371/journal.pone.0051334.
[37] Y. Brito-Casillas, C. Melián, A.M. Wägner, Study of the pathogenesis and treatment of diabetes mellitus through animal models, Endocrinol. Y. Nutr. *63* (2016) 345–353, https://doi.org/10.1016/j.endonu.2016.03.011.
[38] D.E. Chusyd, D. Wang, D.M. Huffman, T.R. Nagy, Relationships between rodent white adipose fat pads and human white adipose fat depots, Front Nutr. *3* (2016) 10.
[39] I. Gabriely, X.H. Ma, X.M. Yang, G. Atzmon, M.W. Rajala, A.H. Berg, P. Scherer, L. Rossetti, N. Barzilai, Removal of visceral fat prevents insulin resistance and glucose intolerance of aging: an adipokine-mediated process? Diabetes *51* (2002) 2951–2958, https://doi.org/10.2337/diabetes.51.10.2951.
[40] R.G. Peterson, W.N. Shaw, M.-A. Neel, L.A. Little, J. Eichberg, Zucker Diabetic fatty rat as a model for non-insulin-dependent diabetes mellitus, ILAR J. *32* (1990) 16–19, https://doi.org/10.1093/ilar.32.3.16.
[41] B.L. Kasiske, M.P. O'Donnell, W.F. Keane, The zucker rat model of obesity, insulin resistance, hyperlipidemia, and renal injury, Hypertension *19* (1992) I-110–I-115, https://doi.org/10.1161/01.hyp.19.1_suppl.i110.
[42] A. Aleixandre De Artiñano, M. Miguel Castro, Experimental rat models to study the metabolic syndrome, Br. J. Nutr. *102* (2009) 1246–1253.
[43] I.R. Lanza, K.S. Nair, Functional Assessment of isolated mitochondria in vitro, Methods Enzymol. *457* (2009) 349–372.
[44] G. Bartolommei, M.R. Moncelli, F. Tadini-Buoninsegni, A method to measure hydrolytic activity of adenosinetriphosphatases (ATPases), PLoS One *8* (2013) e58615, https://doi.org/10.1371/journal.pone.0058615.
[45] W. Masocha, L.G. González, A. Agil, Distinguishing subgroups among μ-opioid receptor agonists using Na+,K+-ATPase as an effector mechanism, Eur. J. Pharmacol. *774* (2016) 43–49, https://doi.org/10.1016/j.ejphar.2016.01.010.
[46] M. Navarro-Alarcón, F.J. Ruiz-Ojeda, R.M. Blanca-Herrera, M.M. A-Serrano, D. Acuña-Castroviejo, G. Fernández-Vázquez, A. Agil, Melatonin and metabolic regulation: a review, Food Funct. *5* (2014) 2806–2832, https://doi.org/10.1039/c4fo00317a.
[47] A. Agil, I. Rosado, R. Ruiz, A. Figueroa, N. Zen, G. Fernández-Vázquez, Melatonin improves glucose homeostasis in young zucker diabetic fatty rats, J. Pineal Res. *52* (2012) 203–210, https://doi.org/10.1111/j.1600-079X.2011.00928.x.
[48] D. Salagre, M. Chayah, A. Molina-Carballo, M.J. Oliveras-López, A. Munoz-Hoyos, M. Navarro-Alarcón, G. Fernández-Vázquez, A. Agil, Melatonin induces fat browning by transdifferentiation of white adipocytes and de novo differentiation of mesenchymal stem cells, Food Funct. *13* (2022) 3760–3775, https://doi.org/10.1039/d1fo04360a.
[49] S. Aouichat, E. Raya, A. Molina-Carballo, A. Munoz-Hoyos, A.S. Aloweidi, E. K. Elmahallawy, A. Agil, Dose-dependent effect of melatonin on bat thermogenesis in Zücker diabetic fatty rat: future clinical implications for obesity, Antioxidants *11* (2022) 1646, https://doi.org/10.3390/antiox11091646.
[50] A. Agil, M. Navarro-Alarcon, F.A.Z. Ali, A. Albrakati, D. Salagre, C. Campoy, E. K. Elmahallawy, Melatonin enhances the mitochondrial functionality of brown adipose tissue in obese—diabetic rats, Antioxidants *10* (2021) 1482, https://doi.org/10.3390/antiox10091482.
[51] G. Fernández Vázquez, R.J. Reiter, A. Agil, Melatonin increases brown adipose tissue mass and function in zücker diabetic fatty rats: implications for obesity control, J. Pineal Res. *64* (2018) e12472, https://doi.org/10.1111/jpi.12472.
[52] J.D. Sparks, T.L. Phung, M. Bolognino, J. Cianci, R. Khurana, R.G. Peterson, M. P. Sowden, J.P. Corsetti, C.E. Sparks, Lipoprotein alterations in 10- and 20-week-old zucker diabetic fatty rats: hyperinsulinemic versus insulinopenic hyperglycemia, Metabolism *47* (1998) 1315–1324, https://doi.org/10.1016/S0026-0495(98)90298-0.
[53] K. Lum-Naihe, R. Toedebusch, A. Mahmood, J. Bajwa, T. Carmack, S.A. Kumar, S. Ardhanari, V.G. Demarco, C.A. Emter, L. Pulakat, Cardiovascular disease progression in female zucker diabetic fatty rats occurs via unique mechanisms compared to males, Sci. Rep. *7* (2017) 17823, https://doi.org/10.1038/s41598-017-18003-8.
[54] E.S. Park, J.K. Seong, S.J. Yi, J.S. Kim, H.S. Lee, I.S. Lee, Y.S. Yoon, Changes in orexin-A and neuropeptide y expression in the hypothalamus of obese and lean zucker diabetic fatty rats, J. Vet. Med. Sci. *67* (2005) 639–646, https://doi.org/10.1292/jvms.67.639.
[55] C. Gustavsson, T. Soga, E. Wahlström, M. Vesterlund, A. Azimi, G. Norstedt, P. Tollet-Egnell, Sex-dependent hepatic transcripts and metabolites in the development of glucose intolerance and insulin resistance in zucker diabetic fatty rats, J. Mol. Endocrinol. *47* (2011) 129–143, https://doi.org/10.1530/JME-11-0007.
[56] J.P. Corsetti, J.D. Sparks, R.G. Peterson, R.L. Smith, C.E. Sparks, Effect of dietary fat on the development of non-insulin dependent diabetes mellitus in obese zucker diabetic fatty male and female rats, Atherosclerosis *148* (2000) 231–241, https://doi.org/10.1016/S0021-9150(99)00265-8.
[57] N. Vrang, J. Jelsing, L. Simonsen, A.E. Jensen, I. Thorup, H. Søeborg, L. B. Knudsen, The Effects of 13 Wk of liraglutide treatment on endocrine and exocrine pancreas in male and female ZDF rats: a quantitative and qualitative analysis revealing no evidence of drug-induced pancreatitis, Am. J. Physiol. Endocrinol. Metab. *303* (2012) E253–64, https://doi.org/10.1152/ajpendo.00182.2012.
[58] I. Maric, J.P. Krieger, P. van der Velden, S. Börchers, M. Asker, M. Vujicic, I. Wernstedt Asterholm, K.P. Skibicka, Sex and species differences in the development of diet-induced obesity and metabolic disturbances in rodents, Front. Nutr. *9* (2022) 828522, https://doi.org/10.3389/fnut.2022.828522.
[59] B.F. Palmer, D.J. Clegg, The sexual dimorphism of obesity, Mol. Cell Endocrinol. *402* (2015) 113–119.
[60] F.D.S. Pimenta, H. Tose, É.W. Jr, M.R.H. Da Cunha, F.V. Campos, E.C. Vasquez, H. Mauad, Lipectomy associated to obesity produces greater fat accumulation in

the visceral white adipose tissue of female compared to male rats, Lipids Health Dis. *18* (2019) 44, https://doi.org/10.1186/s12944-019-0988-5.
[61] N. Kapoor, S. Arora, S. Kalra, Gender disparities in people living with obesity - an unchartered territory, J. Midlife Health *12* (2021) 103, https://doi.org/10.4103/jmh.jmh_48_21.
[62] A.J. Cooper, S.R. Gupta, A.F. Moustafa, A.M. Chao, Sex/Gender Differences in obesity prevalence, comorbidities, and treatment, *Curr. Obes. Rep. 10* (2021) 458–466.
[63] D.D. Rasmussen, D.R. Mitton, S.A. Larsen, S.M. Yellon, Aging-Dependent changes in the effect of daily melatonin supplementation on rat metabolic and behavioral responses, J. Pineal Res. *31* (2001) 89–94, https://doi.org/10.1034/j.1600-079X.2001.310113.x.
[64] D.D. Rasmussen, B.M. Boldt, C.W. Wilkinson, S.M. Yellon, A.M. Matsumoto, Daily melatonin administration at middle age suppresses male rat visceral fat, plasma leptin, and plasma insulin to youthful levels, Endocrinology *140* (1999) 1009–1012, https://doi.org/10.1210/endo.140.2.6674.
[65] T. Wolden-Hanson, D.R. Mitton, R.L. McCants, S.M. Yellon, C.W. Wilkinson, A. M. Matsumoto, D.D. Rasmussen, Daily melatonin administration to middle-aged male rats suppresses body weight, intraabdominal adiposity, and plasma leptin and insulin independent of food intake and total body fat, Endocrinology *141* (2000) 487–497, https://doi.org/10.1210/endo.141.2.7311.
[66] L. Wang, J.W. McFadden, G. Yang, H. Zhu, H. Lian, T. Fu, Y. Sun, T. Gao, M. Li, Effect of melatonin on visceral fat deposition, lipid metabolism and hepatic lipo-metabolic gene expression in male rats, J. Anim. Physiol. Anim. Nutr. *105* (2021) 787–796, https://doi.org/10.1111/jpn.13497.
[67] B. Prunet-Marcassus, M. Desbazeille, A. Bros, K. Louche, P. Delagrange, P. Renard, L. Casteilla, L. Pénicaud, Melatonin reduces body weight gain in sprague dawley rats with diet-induced obesity, Endocrinology *144* (2003) 5347–5352, https://doi.org/10.1210/en.2003-0693.
[68] G. Favero, A. Stacchiotti, S. Castrezzati, F. Bonomini, M. Albanese, R. Rezzani, L. F. Rodella, Melatonin reduces obesity and restores adipokine patterns and metabolism in obese (Ob/Ob) mice, Nutr. Res. *35* (2015) 891–900, https://doi.org/10.1016/j.nutres.2015.07.001.
[69] R. Sartori, V. Romanello, M. Sandri, Mechanisms of muscle atrophy and hypertrophy: implications in health and disease, Nat. Commun. *12* (2021) 330.
[70] A.M. Mengeste, A.C. Rustan, J. Lund, Skeletal muscle energy metabolism in obesity, *Obesity 29* (2021) 1582–1595.
[71] S.G. Wannamethee, J.L. Atkins, Muscle loss and obesity: the health implications of sarcopenia and sarcopenic obesity, Proc. Nutr. Soc. Vol. 74 (2015) 405–412. November 1.
[72] B. Cousin, S. Cinti, M. Morroni, S. Raimbault, D. Ricquier, L. Penicaud, L. Casteilla, Occurrence of brown adipocytes in rat white adipose tissue: molecular and morphological characterization, J. Cell Sci. *103* (1992) 931–942, https://doi.org/10.1242/jcs.103.4.931.
[73] G. Barbatelli, I. Murano, L. Madsen, Q. Hao, M. Jimenez, K. Kristiansen, J. P. Giacobino, R. De Matteis, S. Cinti, The emergence of cold-induced brown adipocytes in mouse white fat depots is determined predominantly by white to brown adipocyte transdifferentiation, Am. J. Physiol. Endocrinol. Metab. *298* (2010) E1244–53, https://doi.org/10.1152/ajpendo.00600.2009.
[74] W.D. van Marken Lichtenbelt, J.W. Vanhommerig, N.M. Smulders, J.M.A.F. L. Drossaerts, G.J. Kemerink, N.D. Bouvy, P. Schrauwen, G.J.J. Teule, Cold-activated brown adipose tissue in healthy men, New Engl. J. Med. *360* (2009) 1500–1508, https://doi.org/10.1056/nejmoa0808718.
[75] W.S. Smith, R. Broadbridge, J.M. East, A.G. Lee, Sarcolipin uncouples hydrolysis of ATP from accumulation of Ca2+ by the Ca2+-ATPase of skeletal-muscle sarcoplasmic reticulum, Biochem. J. *361* (2002) 277–286, https://doi.org/10.1042/0264-6021:3610277.
[76] S. Mall, R. Broadbridge, S.L. Harrison, M.G. Gore, A.G. Lee, J.M. East, The presence of sarcolipin results in increased heat production by Ca 2+-ATPase, J. Biol. Chem. *281* (2006) 36597–36602, https://doi.org/10.1074/jbc.M606869200.
[77] A. Tremblay, J.P. Chaput, Short communication: adaptive reduction in thermogenesis and resistance to lose fat in obese men, Br. J. Nutr. *102* (2009) 488–492, https://doi.org/10.1017/S0007114508207245.
[78] M. Rosenbaum, R.L. Goldsmith, F. Haddad, K.M. Baldwin, R. Smiley, D. Gallagher, R.L. Leibel, Triiodothyronine and leptin repletion in humans similarly reverse weight-loss-induced changes in skeletal muscle, Am. J. Physiol. Endocrinol. Metab. *315* (2018) E771–E779, https://doi.org/10.1152/ajpendo.00116.2018.
[79] I.A. Hobai, K. Aziz, E.S. Buys, P. Brouckaert, D.A. Siwik, W.S. Colucci, Distinct myocardial mechanisms underlie cardiac dysfunction in endotoxemic male and female mice, Shock *46* (2016) 713–722, https://doi.org/10.1097/SHK.0000000000000679.
[80] D.W. Schwertz, J.M. Beck, J.M. Kowalski, J.D. Ross, Sex differences in the response of rat heart ventricle to calcium, Biol. Res Nurs. *5* (2004) 286–298, https://doi.org/10.1177/1099800403262615.
[81] V. Vachharajani, S. Vital, Obesity and sepsis, J. Intensive Care Med. *21* (2006) 287–295.
[82] M. Pant, N.C. Bal, M. Periasamy, Cold adaptation overrides developmental regulation of sarcolipin expression in mice skeletal muscle: SOS for muscle-based thermogenesis? J. Exp. Biol. *218* (2015) 2321–2325, https://doi.org/10.1242/jeb.119164.
[83] N.C. Bal, S.C. Gupta, M. Pant, D.H. Sopariwala, G. Gonzalez-Escobedo, J. Turner, J.S. Gunn, C.R. Pierson, S.Q. Harper, J.A. Rafael-Fortney, et al., Is upregulation of sarcolipin beneficial or detrimental to muscle function? Front. Physiol. *12* (2021) 633058 https://doi.org/10.3389/fphys.2021.633058.
[84] H. Eshima, Influence of Obesity and type 2 diabetes on calcium handling by skeletal muscle: spotlight on the sarcoplasmic reticulum and mitochondria, Front Physiol. *12* (2021) 758316.
[85] S. Herzig, R.J. Shaw, AMPK: guardian of metabolism and mitochondrial homeostasis, Nat. Rev. Mol. Cell Biol. *19* (2018) 121–135.
[86] J.H. Han, M.T. Kim, C.S. Myung, Garcinia cambogia improves high-fat diet-induced glucose imbalance by enhancing calcium/CaMKII/AMPK/GLUT4-mediated glucose uptake in skeletal muscle, Mol. Nutr. Food Res. *66* (2022) e2100669, https://doi.org/10.1002/mnfr.202100669.
[87] J.S. Son, S.A. Chae, L. Zhao, H. Wang, J.M. de Avila, M.J. Zhu, Z. Jiang, M. Du, Maternal exercise intergenerationally drives muscle-based thermogenesis via activation of apelin-AMPK signaling, EBioMedicine *76* (2022) 103842, https://doi.org/10.1016/j.ebiom.2022.103842.
[88] K. Funai, H. Song, L. Yin, I.J. Lodhi, X. Wei, J. Yoshino, T. Coleman, C. F. Semenkovich, Muscle lipogenesis balances insulin sensitivity and strength through calcium signaling, J. Clin. Investig. *123* (2013) 1229–1240, https://doi.org/10.1172/JCI65726.
[89] Z. Chen, L. Ding, W. Yang, J. Wang, L. Chen, Y. Chang, B. Geng, Q. Cui, Y. Guan, J. Yang, Hepatic activation of the FAM3C-HSF1-CaM pathway attenuates hyperglycemia of obese diabetic mice, Diabetes *66* (2017) 1185–1197, https://doi.org/10.2337/db16-0993.
[90] E. Avelar, T.V. Cloward, J.M. Walker, R.J. Farney, M. Strong, R.C. Pendleton, N. Segerson, T.D. Adams, R.E. Gress, S.C. Hunt, et al., Left Ventricular hypertrophy in severe obesity: interactions among blood pressure, nocturnal hypoxemia, and body mass, Hypertension *49* (2007) 34–39, https://doi.org/10.1161/01.HYP.0000251711.92482.14.
[91] M. Prévilon, M. Pezet, L. Vinet, J.J. Mercadier, P. Rouet-Benzineb, Gender-specific potential inhibitory role of Ca2+/calmodulin dependent protein kinase phosphatase (CaMKP) in pressure-overloaded mouse heart, PLoS One *9* (2014) e90822, https://doi.org/10.1371/journal.pone.0090822.
[92] R.J. Parks, S.E. Howlett, Sex differences in mechanisms of cardiac excitation-contraction coupling, Pflug. Arch. *465* (2013) 747–763.
[93] R.K. Devulapalli, J.L. Nelsen, S.A. Orsi, T. McFadden, S. Navabpour, N. Jones, K. Martin, M. O'Donnell, E.L. McCoig, T.J. Jarome, Males and females differ in the subcellular and brain region dependent regulation of proteasome activity by CaMKII and protein kinase A, Neuroscience *418* (2019) 1–14, https://doi.org/10.1016/j.neuroscience.2019.08.031.
[94] K. Mizuno, A. Antunes-Martins, L. Ris, M. Peters, E. Godaux, K.P. Giese, Calcium/calmodulin kinase kinase β has a male-specific role in memory formation, Neuroscience *145* (2007) 393–402, https://doi.org/10.1016/j.neuroscience.2006.11.056.
[95] D. Watanabe, K. Hatakeyama, R. Ikegami, H. Eshima, K. Yagishita, D.C. Poole, Y. Kano, Sex differences in mitochondrial Ca2+ handling in mouse fast-twitch skeletal muscle in vivo, J. Appl. Physiol. *128* (2020) 241–251, https://doi.org/10.1152/japplphysiol.00230.2019.
[96] A. Ciocci Pardo, G.J. Rinaldi, S.M. Mosca, Data supporting the cardiac mitochondria calcium handling in female normotensive and spontaneously hypertensive rats, Data Brief. *7* (2016) 406–410, https://doi.org/10.1016/j.dib.2016.02.056.
[97] T.E. Claessens, E.R. Rietzschel, M.L. De Buyzere, D. De Bacquer, G. De Backer, T. C. Gillebert, P.R. Verdonck, P. Segers, Noninvasive assessment of left ventricular and myocardial contractility in middle-aged men and women: disparate evolution above the Age of 50? Am. J. Physiol. Heart Circ. Physiol. *292* (2007) H856–65, https://doi.org/10.1152/ajpheart.00759.2006.
[98] K. Benchoula, A. Mediani, W.E. Hwa, The functions of Ca2+/calmodulin-dependent protein kinase II (CaMKII) in diabetes progression, J. Cell. Commun. Signal. *17* (2023) 25–34.
[99] J.S. Joseph, K. Anand, S.T. Malindisa, O.F. Fagbohun, Role of CaMKII in the regulation of fatty acids and lipid metabolism, Diabetes Metab. Syndr.: Clin. Res. Rev. *15* (2021) 589–594.
[100] J.N. Williams, U. Sankar, CaMKK2 Signaling in metabolism and skeletal disease: a new axis with therapeutic potential, Curr. Osteoporos. Rep. *17* (2019) 169–177.
[101] B.G. Teodoro, F.G. Baraldi, I.H. Sampaio, L.H.M. Bomfim, A.L. Queiroz, M. A. Passos, E.M. Carneiro, L.C. Alberici, R. Gomis, F.G. Amaral, et al., Melatonin prevents mitochondrial dysfunction and insulin resistance in rat skeletal muscle, J. Pineal Res. *57* (2014) 155–167, https://doi.org/10.1111/jpi.12157.
[102] C. Mendes, A.M.D.S. Lopes, F.G. Do Amaral, R.A. Peliciari-Garcia, A.D.O. Turati, S.M. Hirabara, J.H. Scialfa Falcão, J. Cipolla-Neto, Adaptations of the aging animal to exercise: role of daily supplementation with melatonin, J. Pineal Res. *55* (2013) 229–239, https://doi.org/10.1111/jpi.12065.
[103] L. Xu, D. Li, H. Li, O. Zhang, Y. Huang, H. Shao, Y. Wang, S. Cai, Y. Zhu, S. Jin, et al., Suppression of obesity by melatonin through increasing energy expenditure and accelerating lipolysis in mice fed a high-fat diet, Nutr. Diabetes *12* (2022) 42, https://doi.org/10.1038/s41387-022-00222-2.
[104] J.S. Joseph, A.O. Ayeleso, E. Mukwevho, Role of exercise-induced calmodulin protein kinase (CaMK)II activation in the regulation of omega-6 fatty acids and lipid metabolism genes in rat skeletal muscle, Physiol. Res. *66* (2017) 969–977, https://doi.org/10.33549/physiolres.933509.
[105] S. Tomiya, Y. Tamura, K. Kouzaki, T. Kotani, Y. Wakabayashi, M. Noda, K. Nakazato, Cast immobilization of hindlimb upregulates sarcolipin expression in atrophied skeletal muscles and increases thermogenesis in C57BL/6J mice, Am. J. Physiol. Regul. Integr. Comp. Physiol. *317* (2019) R649–R661, https://doi.org/10.1152/ajpregu.00118.2019.
[106] A.R. Martins, A.R. Crisma, L.N. Masi, C.L. Amaral, G.N. Marzuca-Nassr, L.H. M. Bomfim, B.G. Teodoro, A.L. Queiroz, T.D.A. Serdan, R.P. Torres, et al., Attenuation of obesity and insulin resistance by fish oil supplementation is

associated with improved skeletal muscle mitochondrial function in mice fed a high-fat diet, J. Nutr. Biochem. *55* (2018) 76–88, https://doi.org/10.1016/j.jnutbio.2017.11.012.

[107] M. Moriggi, S. Belloli, P. Barbacini, V. Murtaj, E. Torretta, L. Chaabane, T. Canu, S. Penati, M.L. Malosio, A. Esposito, et al., Skeletal muscle proteomic profile revealed gender-related metabolic responses in a diet-induced obesity animal model, Int. J. Mol. Sci. *22* (2021) 4680, https://doi.org/10.3390/ijms22094680.

[108] S.F. Martinez-Huenchullan, B.R. Maharjan, P.F. Williams, C.S. Tam, S. V. Mclennan, S.M. Twigg, Skeletal muscle adiponectin induction depends on diet, muscle type/activity, and exercise modality in C57BL/6 Mice, Physiol. Rep. *6* (2018) e13848, https://doi.org/10.14814/phy2.13848.

[109] K.M. Haizlip, B.C. Harrison, L.A. Leinwand, Sex-based differences in skeletal muscle kinetics and fiber-type composition, Physiology *30* (2015) 30–39.

[110] C. Cantó, J. Auwerx, PGC-1α, SIRT1 and AMPK, an energy sensing network that controls energy expenditure, Curr. Opin. Lipido *20* (2009) 98–105.

[111] T. Akimoto, T.J. Ribar, R.S. Williams, Z. Yan, Skeletal Muscle Adaptation in response to voluntary running in Ca 2+/calmodulin-dependent protein kinase IV-deficient mice, Am. J. Physiol. Cell Physiol. *287* (2004) C1311–9, https://doi.org/10.1152/ajpcell.00248.2004.

[112] M.G. Akl, L. Li, R. Baccetto, S. Phanse, Q. Zhang, M.J. Trites, S. McDonald, H. Aoki, M. Babu, S.B. Widenmaier, Complementary gene regulation by NRF1 and NRF2 protects against hepatic cholesterol overload, Cell Rep. *42* (2023) 112399, https://doi.org/10.1016/j.celrep.2023.112399.

[113] M.M. Rahman, H.S. Kwon, M.J. Kim, H.K. Go, M.H. Oak, D.H. Kim, Melatonin supplementation plus exercise behavior ameliorate insulin resistance, hypertension and fatigue in a rat model of type 2 diabetes mellitus, Biomed. Pharmacother. *92* (2017) 606–614, https://doi.org/10.1016/j.biopha.2017.05.035.

[114] A. Shabani, F. Foroozanfard, E. Kavossian, E. Aghadavod, V. Ostadmohammadi, R.J. Reiter, T. Eftekhar, Z. Asemi, Effects of Melatonin administration on mental health parameters, metabolic and genetic profiles in women with polycystic ovary syndrome: a randomized, double-blind, placebo-controlled trial, J. Affect. Disord. *250* (2019) 51–56, https://doi.org/10.1016/j.jad.2019.02.066.

[115] W. Chen, Y. Tu, P. Cai, L. Wang, Y. Zhou, S. Liu, Y. Huang, S. Zhang, X. Gu, W. Yi, et al., Melatonin supplementation promotes muscle fiber hypertrophy and regulates lipid metabolism of skeletal muscle in weaned piglets, J. Anim. Sci. *101* (2023) skad256, https://doi.org/10.1093/jas/skad256.

[116] C.A. Pileggi, G. Parmar, M.E. Harper, The lifecycle of skeletal muscle mitochondria in obesity, Obes. Rev. *22* (2021) e13164.

[117] A.C. Smith, K.L. Mullen, K.A. Junkin, J. Nickerson, A. Chabowski, A. Bonen, D. J. Dyck, Metformin and exercise reduce muscle FAT/CD36 and lipid accumulation and blunt the progression of high-fat diet-induced hyperglycemia, Am. J. Physiol. Endocrinol. Metab. *293* (2007) E172–81, https://doi.org/10.1152/ajpendo.00677.2006.

[118] A. Agil, M. El-Hammadi, A. Jiménez-Aranda, M. Tassi, W. Abdo, G. Fernández-Vázquez, R.J. Reiter, Melatonin reduces hepatic mitochondrial dysfunction in diabetic obese rats, J. Pineal Res. *59* (2015) 70–79, https://doi.org/10.1111/jpi.12241.